TABLE III. Data for particles lighter than a μ meson.

Label in Fig. 1	Sign of charge	Mean magnetic field in gauss Hm	Thickness in g/cm² and material of plate D	Inverse momentum in c/Mev $\Phi_1=1/P_1$ $(\Phi_1\pm\Delta\Phi_1)\times100$	Threshold inverse momentum in c/Mev $\Phi_0\times100$	Deviation of inverse momentum in units of $\Delta\Phi_1$ $(\Phi_1-\Phi_0)/\Delta\Phi_1$	Ionization in units of minimum ionization $I_1\pm\Delta I_1$	Deviation of ionization[a] in units of ΔI_0 $(I_1-I_0)/\Delta I_0$	Upper limit of mass in units of electron mass $<M(P_1R)$
α	−	2050	0.92, C	2.52±0.14	2.07	3.2	2.0±0.2	4.0	172+14
β	−	2100	0.93, C	2.59±0.14	2.04	4.6	2.2±0.3	5.0	166+13
γ	−	1510	0.35, Al	4.14±0.19	2.94	6.3	2.5±0.3	6.5	131+9
δ	+	1490	0.14, Al	10.31±0.33	3.86	19.5	2.1±0.3	4.5	51+2

[a] The average ionization of the electron is taken to be 1.2 times the minimum. The probable error of a single observation of the ionization is taken to be 0.2 in the same units.

identified as lighter mesons, unless they are more densely ionizing ones. Thus they may be electrons, but the possibility that some of them are lighter mesons is not excluded.

When one compares this result with that previously described, the relative intensity of unidentified particles to μ mesons is exceedingly reduced in this study.

The authors wish to thank Mr. Tsushima and Mr. Onuma for their collaboration in constructing and operating the apparatus.

PHYSICAL REVIEW VOLUME 105, NUMBER 6 MARCH 15, 1957

Isobaric Nucleon Model for Pion Production in Nucleon-Nucleon Collisions*

S. J. LINDENBAUM AND R. M. STERNHEIMER
Brookhaven National Laboratory, Upton, New York

(Received December 13, 1956)

A detailed quantitative model for pion production via excitation of one or both nucleons to an isobaric state with subsequent decay via pion emission is presented. The model is applied to the 0.8- to 3.0-Bev incident nucleon energy range and its predictions are compared to various experiments in this energy range performed at the Brookhaven Cosmotron. The isobaric state with isotopic spin and angular momentum $=\frac{3}{2}$ observed in the pion-nucleon scattering was assumed to be predominantly responsible for pion production in this energy range. The relative probability for isobar formation and subsequent decay with a variable total energy or mass in the isobar rest system were phenomenologically related to the π^+-p interaction cross section. The energy or momentum spectra of pions, and nucleons, the variation of the ratio of double to single production, the angular correlation, and the Q value distribution for pion-nucleon pairs have been calculated at various energies from 0.8- to 3.0-Bev and generally agree with the experimental results.

I. INTRODUCTION

THE early cosmic-ray studies[1] of pion production by incoming nucleons with energies ranging from 1 to ~100 Bev had been found generally consistent with the statistical theory which was proposed by Fermi[2] to explain them. The essential features of this theory were that a thermodynamic equilibrium was assumed to be established inside a collision volume of radius equal to to the pion Compton wavelength and then the relative probability of a final state—with n pions of momenta $(p_1,p_2\cdots p_n)$ and 2 nucleons (p_{n+1},p_{n+2}), was considered to be proportional to the phase space available for this state. Hence it was assumed that the matrix elements for all final states were essentially the same. The only final states which were applicable were, of course, those which conserved charge, energy, momentum, angular momentum, heavy particles, and isotopic spin.

The energy spectra and other characteristics of pion production in Be and hydrogen by 1.0- to 3.0-Bev protons were observed by Lindenbaum and Yuan[3] using the Brookhaven Cosmotron. These results did not agree with the predictions of the Fermi statistical theory which were calculated by Yang and Christian.[4] Over the incident proton energy range of 1.0–2.3 Bev, the observed experimental pion energy spectra in the

* Work performed under the auspices of the U. S. Atomic Energy Commission.

[1] B. Rossi, *High-Energy Particles* (Prentice-Hall, Inc., New York, 1952), Chap. VIII.

[2] E. Fermi, Progr. Theoret. Phys. (Japan) **5**, 570 (1950); Phys. Rev. **92**, 452 (1953); **93**, 1435 (1954).

[3] S. J. Lindenbaum and L. C. L. Yuan, Phys. Rev. **93**, 917 and 1431 (1954); **103**, 404 (1956); *Proceedings of the Fourth Annual Rochester Conference on High-Energy Physics* (Interscience Publishers, Inc., New York, 1954), p. 140; *Proceedings of the Fifth Annual Rochester Conference on High-Energy Physics* (Interscience Publishers, Inc., New York, 1955), p. 531; *Proceedings of the Sixth Annual Rochester Conference on High-Energy Physics* (Interscience Publishers, Inc., New York, 1956), Chap. IV, p. 37.

[4] C. N. Yang and R. S. Christian, Brookhaven National Laboratory Internal Report (1953) (unpublished).

nucleon-nucleon center-of-mass system (hereafter abbreviated to c.m.s.) were all similar in shape to the $\pi^+ + p$ scattering cross section as a function of energy with a characteristic low-energy peak at ~100–200 Mev. Furthermore the multiplicity was deduced from the π^+/π^- ratios and conservation of energy requirement to change from essentially single production below 1 Bev to predominantly double production at 2.3 Bev, while the energy spectrum remained essentially similar in shape.

The Fermi statistical theory predicted much less double production and a great change in energy spectrum shape from single to double production. The greater multiplicity observed at 2.3 Bev could have been obtained in the Fermi theory by increasing the interaction radius sufficiently. This would also have led to a change in the right direction for the energy spectrum, since the double production spectrum is closer in shape to the experimental one. However, the result is still quite different from the experimental energy spectra. Furthermore this yields a total cross section or interaction range estimate which is much greater than that observed. Another major difficulty was that especially at 1.0 Bev where double production is negligible there were too many low-energy pions in the experimental results when compared to the Fermi theory.

This observation led Lindenbaum and Yuan[3] to conclude that the strong pion-nucleon interaction previously observed in the pion nucleon scattering completely dominates the production process, and suggests that the pion production proceeds predominantly via the excitation of one or both nucleons to the isobaric state with isotopic spin (T) and angular momentum (J)$=\frac{3}{2}$.

Peaslee[5] then deduced the ratios π^+, π^-, and π^0 mesons expected for either single or double production via this isobar by applying conservation of isotopic spin. Peaslee's ratios have been compared with the above and various other experiments,[5–8] and agree much better than the corresponding values deduced from the Fermi theory. Several cloud chamber experiments by Brookhaven groups[6,7] have also revealed much better agreement with the isobar model than with the Fermi statistical theory.

A modified statistical theory calculation by Kovacs[9] in which the final state pion-nucleon interaction was taken into account has also yielded reasonable branching ratios for various charge states, π^+/π^- ratios, and predictions for the behavior of the multiplicity as a function of energy. This procedure, of course, tends to improve considerably the statistical theory predictions since it essentially includes the resonance interaction in the final state.

Lepore and Neuman[10] have proposed a statistical theory in which the phase space volume accessible to a particle decreases with increasing energy. This energy dependence of the volume was introduced to conserve the relativistic center of energy (relativistic analog of center of mass). The resultant discrimination against high-energy pions tends to provide momentum spectra with a much lower energy peak than the Fermi theory especially for single production, and hence tends to agree with the experimentally observed spectra.

In the present paper a detailed quantitative model for the calculation of the production of one or two nucleon isobars in a nucleon-nucleon collision is presented. The relative probability for a final state is taken to be proportional to the final two-body phase space factor multiplied by the relative probability for formation of one or two $T=\frac{3}{2}$ isobars. The mass of each isobar was considered variable and equal to the total energy in the center-of-mass system of the pion and nucleon resulting from the isobar decay. The probability for isobar formation has previously been related to the observed total $(\pi^+ + p)$ scattering cross section and this expression[11] is employed.

The angular distribution of the isobars produced was considered for two cases: isotropic, and only forward and backward in the c.m.s. The decay pions were assumed to be isotropically emitted in the rest system of the decaying isobar in both cases. Although more detailed assumptions can be made for the angular distributions, mixtures of the present ones are entirely adequate to fit the observed experimental data. The ratio of double production to the sum of single and double production in a single isotopic spin state depends in this theory on only one constant k for which a single value provides an adequate fit for the experimental data throughout the range 1.0- to 3.0-Bev in p-p collisions.

The conservation of T and T_z is assumed throughout the process. The decomposition of the initial two-nucleon state characterized by a particular T and T_z into one or two isobars of $T'=\frac{3}{2}$ and various allowed T_z' is weighted according to the appropriate Clebsch-Gordan coefficients. Furthermore the proper weights for the decay of the isobars into π^+, π^0, π^- mesons are included to obtain the individual properties of these mesons.

The calculations were carried out for 0.8-, 1.0-, 1.5-, 2.3-, and 3.0-Bev incident nucleon energy. The calculated results fit the data which is available at present quite well.

[5] D. C. Peaslee, Phys. Rev. **94**, 1085 (1954); **95**, 1580 (1954).
[6] Fowler, Shutt, Thorndike, and Whittemore, Phys. Rev. **95**, 1026 (1954).
[7] Morris, Fowler, and Garrison, Phys. Rev. **103**, 1472 (1956); Fowler, Shutt, Thorndike, and Whittemore, Phys. Rev. **103**, 1479 (1956); M. M. Block *et al.*, Phys. Rev. **103**, 1484 (1956); W. B. Fowler *et al.*, Phys. Rev. **103**, 1489 (1956). These papers will be referred to as 7(I), 7(II), 7(III), and 7(IV), respectively.
[8] Cester, Hoang, and Kernan, Phys. Rev. **103**, 1443 (1956).
[9] J. S. Kovacs, Phys. Rev. **101**, 397 (1956).
[10] J. V. Lepore and M. Neuman, Phys. Rev. **98**, 1484 (1955).
[11] See footnote 16 on p. 409 of L. C. L. Yuan and S. J. Lindenbaum, Phys. Rev. **103**, 404 (1956).

II. ISOBARIC NUCLEON MODEL

The strong-coupling theory of the meson-nucleon system predicts a series of nucleon isobaric levels above the nucleon ground state.[12] In such a picture one would expect the pion-nucleon interaction cross section to exhibit a series of resonant isobaric energy levels. An analysis of the pion-hydrogen interaction cross sections[13] supports the view that such an isobar exists in the $T'=J=\frac{3}{2}$ state. Furthermore it appears that for pion kinetic energies in the laboratory system of $\lesssim$200–300 Mev the $T'=J=\frac{3}{2}$ state isobar essentially predominates in the pion-nucleon interaction. The $T'=\frac{1}{2}$ cross section rises from essentially zero at ~200-Mev pion kinetic energy in the laboratory system to a value equal to that of the $T'=\frac{3}{2}$ cross section at ~450-Mev pion kinetic energy in the laboratory system. There is at present no evidence for a bound pion-nucleon state.

One can now consider a series of resonant isobaric levels as characteristic of the internal structure of a nucleon. Hence one can conceive of meson production in a nucleon-nucleon collision as follows:

(1) As a result of the collision there is a transfer of kinetic energy to the internal structure of one or both nucleons. This raises one or both nucleons to one of their set of isobaric levels.

(2) An excited isobar does not interact with the other nucleon or isobar as the case may be, except for the initial transfer of energy and momentum.

(3) The lifetime of the isobars is long enough to allow them to separate before decaying and therefore final state interactions between the decay products of one isobar and the other nucleon or isobar in the collision are small.

We further propose to assume that the dominant isobaric level in the 1.0- to 3.0-Bev incident energy range is the $T'=J=\frac{3}{2}$ state. This assumption has been previously successful in explaining many of the qualitative and some quantitative features of the experimental results.[3] Some further support for this assumption is derived from the work of Henley and Lee[14] who have applied the symmetrical scalar meson theory to the production process and have found that the dominant contribution to the pion production in the Bev range is likely to come from the $T'=\frac{3}{2}$ state with relatively little from the $T'=\frac{1}{2}$ state. Lee[15] expects that this result will also occur for the pseudoscalar case which is being calculated.

Assumption (3) is rather questionable since a calculation of the order of magnitude of the lifetime of the $T'=J=\frac{3}{2}$ state from the observed width gives $\sim10^{-23}$ sec which means that the isobar could still be within the interaction volume (radius $\sim10^{-13}$ cm) at the time of decay. Obviously the agreement or lack of agreement of the model with experiment will be a test of the usefulness of this concept.

However, one might point out that the velocities of the isobars and recoil nucleons are considerable in the 1.0- and 3.0-Bev energy region considered here. Hence if a pion which results from the decay of an isobar has the right relative energy to be strongly interacting with its associated nucleon (i.e., a relative energy near the peak of the $\pi^+ + p$ scattering cross section), its energy relative to the other recoil nucleon or decay nucleon from a second isobar will in general be at a much lower or higher energy. Therefore, its interaction with the second nucleon will be much smaller even if the isobar decays rapidly.[16] Therefore even for a relatively short lifetime some of the dominant features of the present model might still be approximately justified.

In this model single pion production occurs when one nucleon in a nucleon-nucleon collision is excited to the isobar with $T'=J=\frac{3}{2}$ and subsequently decays. In addition to T' and T_z' the isobar is further characterized by the total energy of its decay products in its rest system or equivalently a mass in its rest system denoted by m_i. Let us assume that the π-nucleon interaction proceeds entirely by formation of the $T'=J=\frac{3}{2}$ isobar. Then we can by the following arguments relate the cross section for isobar formation in a nucleon-nucleon collision to the observed $\pi^+ + p$ total interaction cross section which is the $T'=\frac{3}{2}$ state cross section.

We can write the general relation between cross sections and matrix elements as follows:

$$\sigma_{\pi^+ + p}(m_i) = \text{const} \times |M_{\text{isobar}}|_{m_i}^2 \rho(m_i) = \sigma_I(m_i), \quad (1)$$

where m_i is the total energy in the isobar c.m.s. or equivalently the isobar mass; $|M_{\text{isobar}}|_{m_i}$ is the matrix element for isobar formation; $\rho(m_i)$ is the density of final isobar states per unit energy as a function of m_i; $\sigma(m_i)$ is the cross section for isobar formation as a function of m_i and is equal to $\sigma_{\pi^+ + p}(m_i)$.

Let us now consider the case in the π-nucleon interaction where the incident pion beam does not have a unique energy corresponding to a definite value of m_i, but instead a rather wide distribution of energies specified by an arbitrary function $F(m_i)$. Clearly, there will now be a resultant distribution of the mass values of the isobars formed, and the resultant relative cross section per unit mass interval as a function of m_i can now be defined as dP_I/dm_i. It is obvious from Eq. (1)

[12] W. Pauli and S. M. Dancoff, Phys. Rev. **62**, 85 (1942); R. Serber and S. M. Dancoff, Phys. Rev. **63**, 143 (1943).

[13] De Hoffmann, Metropolis, Alei, and Bethe, Phys. Rev. **95**, 1586 (1954); K. A. Brueckner, Phys. Rev. **86**, 106 (1952); S. J. Lindenbaum and L. C. L. Yuan, Phys. Rev. **100**, 306 (1955); Ashkin, Blaser, Feiner, Gorman, and Stern, Phys. Rev. **96**, 1104 (1954); Mukhin, Ozerov, Pontecorvo, Grigoryev, and Mitin, *Proceedings of the International Conference on Peaceful Uses of Atomic Energy* (United Nations, New York, 1956), Vol. II.

[14] E. M. Henley and T. D. Lee, Phys. Rev. **101**, 1536 (1956).

[15] T. D. Lee (private communication).

[16] The nucleon-nucleon final state interaction at these energies is estimated to be small. The possibility of pion-pion final state interaction in the case of double isobar decay is not considered since there is very little evidence for such an interaction.

and the definition of $F(m_i)$ that

$$dP_I(m_i)/dm_i = \text{const} F(m_i)\sigma_I(m_i). \quad (2)$$

In a nucleon-nucleon collision which excites one nucleon to the isobar state, the excitation energy or mass m_i can vary over a wide range consistent with the conservation of energy. Although Eq. (2) has been derived for π-nucleon interactions, one can make the further assumption that in a nucleon-nucleon collision resulting in the excitation of an isobar, a similar form holds for dP_I/dm_i, namely that

$$dP_I/dm_i = \text{const} F(\bar{E},m_i)\sigma_I(m_i), \quad (3)$$

where $\bar{E}$ is the total energy in the c.m.s. of the colliding nucleons. This is equivalent to assuming that the intrinsic probability for isobar formation, which is denoted by the factor $\sigma_I(m_i) = |M_{\text{isobar}}|_{m_i}{}^2\rho(m_i)$ depends only on m_i and not on whether the excitation energy m_i is derived via bombardment by a pion or another nucleon.

The other factor in Eq. (3), $F(\bar{E},m_i)$ is analogous to the factor $F(m_i)$ in the π-nucleon case, and represents the intrinsic distribution of excitation energies available to form the isobar, which results from the details of the nucleon-nucleon collision. A relationship between the cross section for isobar formation and the $\pi^+ + p$ total interaction cross section similar to Eq. (3) has been derived in a previous publication.[11]

Now consider the case where the width of the isobar state $\Gamma \to 0$ or equivalently $m_i \to$ a constant $= m_0$, and $\int \sigma_I(m_i)dm_i \to \text{constant} \times \int \delta(m_i - m_0)dm_i$. Then if we integrate Eq. (3) to obtain the total cross section for isobar formation with a definite mass m_0, it follows that

$$\begin{aligned} P_I(m_0) &= \int \frac{dP_I(m_i)}{dm_i} dm_i \\ &= \text{const} \int F(\bar{E},m_i)\sigma_I(m_i)dm_i, \\ &= \text{const} \int F(\bar{E},m_i)\delta(m_i - m_0)dm_i, \\ &= \text{const} F(\bar{E},m_0). \end{aligned} \quad (4)$$

In this case $\sigma_I(m_0)$ is the cross section for formation of a two-body final state with one body a nucleon and the other a particle of mass m_0. The simplest assumption is that $F(\bar{E},m_0)$ is the two-body phase space factor corresponding to a nucleon and a second particle of mass m_0, for the case where $\bar{E}$ is the total energy in the c.m.s. Therefore in considering the case of a variable mass m_i it is reasonable to consider $F(\bar{E},m_i)$ to be the two-body phase space factor corresponding to $\bar{E}$ and m_i.

The concept of a variable well-defined mass for the isobar is only meaningful a long time after the collision ($t \gg 10^{-23}$ sec) and well outside the collision region ($R \gg$ nucleon range). The mass has been previously defined as the total energy of the final state π-nucleon system resulting from the isobar decay. The treatment of the mass as variable and well-defined in or near the collision region is unjustified. However, this semiclassical approach may still be expected to yield the dominant features of the interaction, provided the resonant interaction of pion and nucleon constituting the isobar is not essentially affected by interference terms due to the presence of the second nucleon in or near the collision volume. Of course, as previously stated, the longer the actual lifetime of the isobar the better this assumption will be.

In the case of double pion production via excitation of both nucleons to isobar levels, we can develop arguments analogous to the single production case to support the following form of the differential cross section for formation of two isobars with masses in the intervals dm_1 about m_1 and dm_2 about m_2:

$$d^2\sigma_{\text{double}}/dm_1dm_2 = F(\bar{E},m_1,m_2)\sigma_I(m_1)\sigma_I(m_2), \quad (5)$$

where $F(\bar{E},m_1,m_2)$ is the two-body phase space factor corresponding to m_1 and m_2 for a total energy $\bar{E}$ in the c.m.s. of the colliding nucleons.

Equations (3) and (5) for single and double pion production respectively refer to the cross sections for isobar formation integrated over all angles in the original nucleon-nucleon c.m.s. Obviously the constants contain an integration over an arbitrary angular distribution and hence Eqs. (3) and (5) can be put in the following form:

$$d\sigma_{\text{single}}/dm_1 = \text{const} \times F(\bar{E},m_1)\sigma(m_1)a_s(\bar{\theta})d\bar{\Omega}, \quad (6)$$

$$d^2\sigma_{\text{double}}/dm_1dm_2 = \text{const} \times F(\bar{E},m_1,m_2)\sigma(m_1) \times \sigma(m_2)dm_1dm_2a_d(\bar{\theta})d\bar{\Omega}, \quad (7)$$

where $a_s(\bar{\theta})$ and $a_d(\bar{\theta})$ are arbitrary functions of $\bar{\theta}$.

The initial two-nucleon state is characterized by a T and T_z which are conserved. This initial state is decomposed into one or two isobars of $T' = \frac{3}{2}$ and various allowed T_z'. These various states are then weighted according to the appropriate Clebsch-Gordan coefficients, and the appropriate weights for the decay of the isobars into π^+, π^0, and π^- mesons are included to obtain the individual properties of these mesons.

The two-body phase space factor is given by[17]

$$F = \bar{p}_1\bar{E}_1\bar{E}_2/\bar{E}, \quad (8)$$

where $\bar{E}$ is the total energy in the c.m.s. of the initial nucleons. In the following, all quantities pertaining to this c.m.s. will be barred. In Eq. (8), $\bar{p}_1$ is the momentum of either particle (N or N^*) in the c.m.s., $\bar{E}_1$ and $\bar{E}_2$ are the total c.m.s. energies of particles 1 and 2, respectively, so that $\bar{E} = \bar{E}_1 + \bar{E}_2$.

The preceding discussion [see Eqs. (6) and (7)], suggests the following expression for the differential

[17] It is assumed that the units are such that $c = 1$.

cross section in the c.m.s. for the production of pions (of all charge states) of kinetic energy $\bar{T}_\pi$, which originate from p-p collisions (total isotopic spin $T=1$):

$$\frac{d^2\sigma}{d\bar{T}_\pi d\bar{\Omega}_\pi}=A\left[\int_{M_a}^{M_2} dm_2 \int_{M_a}^{M_{1,d}} \sigma(m_1)\sigma(m_2)FG_\pi dm_1 + kN\int_{M_a}^{M_{1,s}} \sigma(m_1)FG_\pi dm_1\right], \quad (9)$$

where A is a constant, which merely determines the total inelastic cross section, $G_\pi(m_1,\bar{T}_\pi)$ is a factor giving the energy distribution of the pions emitted into the solid angle $d\bar{\Omega}_\pi$ by the isobar of mass m_1, having total energy $\bar{E}_1$; the parameter k determines the ratio of double to single N^* production. Aside from the factor A, for the case of p-p collisions, which involve only the $T=1$ state, k is the only adjustable constant in the present model. Its value will be obtained below from a comparison of the calculations with the observed pion multiplicity as a function of the incident proton energy. In Eq. (9), N is a normalization constant which is introduced merely in order that the constant k be dimensionless. N is given by

$$N=\int_{M_a}^{M_b}\sigma(m)dm. \quad (9a)$$

In Eqs. (9) and (9a), M_a is the total energy corresponding to a pion at rest in the c.m.s.: $M_a=m_p+m_\pi=1.08$ Bev. The upper limit M_b of Eq. (9a) is $M_b\equiv 1.58$ Bev, corresponding to an excitation energy of 500 Mev plus a pion rest mass. In Eq. (9), the upper limits $M_{1,d}$ and M_2 for double production are defined as follows: $M_{1,d}=\bar{E}-m_2$ or M_b, whichever has the smaller value. Similarly, M_2 is taken as the smaller of the two energies $\bar{E}-M_a$ and M_b. For single production, the upper limit $M_{1,s}$ is the smaller of the two values $\bar{E}-m_p$ and M_b.

Concerning these upper limits in Eq. (9), we note that we are using a cutoff[18] for the isobar mass m_1 (and m_2) at M_b. For the π^+-p system, $M_b=1.58$ Bev corresponds to a 700 Mev-pion in the laboratory system. This cutoff was used because already at 450-Mev laboratory energy; the cross section $\sigma(T'=\frac{1}{2})$ for the pion-nucleon system in the $T'=\frac{1}{2}$ state becomes larger than $\sigma(T'=\frac{3}{2})$ [which is equal to $\sigma(\pi^+-p)$]. The wide maximum of $\sigma(T=\frac{1}{2})$ with center at $\sim$900 Mev extends down to $\sim$700 Mev. Hence it was necessary to use a cutoff at an energy in this region, since the $T'=\frac{1}{2}$ state predominates for higher energies. The use of the cutoff in the present model is expected to result in an underestimate of the high-energy tail of the pion distribution. However, the corresponding error is probably unimportant, since the predominant contribution to the pion production in the 0.8- to 3.0-Bev incident energy range is due to pions which have been made via the $T'=J=\frac{3}{2}$ resonant state, and whose energy is considerably lower than the cutoff.

In Eq. (9), G_π depends, of course, on the angular distribution of the isobars, $a(\bar{\theta}_{N^*})$, where $\bar{\theta}_{N^*}$ is the c.m.s. angle of the isobar with respect to the direction of the incident nucleon. G_π is given by

$$G_\pi(\bar{E}_\pi,m_1)=\int_0^\pi\int_0^{2\pi} a(\bar{\theta}_{N^*})J(\bar{\theta}_\pi)\delta(\bar{E}_\pi-\bar{E}_{\pi,0}) \times\sin\bar{\theta}_{N^*}d\bar{\theta}_{N^*}d\bar{\varphi}_{N^*}, \quad (10)$$

where $J(\bar{\theta}_\pi)$ is the Jacobian for the decay of m_1, $\bar{\theta}_\pi$ is the c.m.s. angle between the directions of motion of the isobar and the emitted pion, $\bar{E}_{\pi,0}$ is the total c.m.s. energy of the pion emitted by the isobar of mass m_1, with energy $\bar{E}_1$, at an angle $\bar{\theta}_\pi$ to the direction of the isobar; $\bar{\varphi}_{N^*}$ is the azimuthal angle of the isobar. We note that $\bar{\theta}_\pi$ is related as follows to $\bar{\theta}_{N^*}$ and to the c.m.s. angle $\bar{\beta}_\pi$ of the pion with respect to the incident nucleon:

$$\cos\bar{\theta}_\pi=\cos\bar{\beta}_\pi\cos\bar{\theta}_{N^*}+\sin\bar{\beta}_\pi\sin\bar{\theta}_{N^*}\cos(\bar{\varphi}_{N^*}-\bar{\varphi}_\pi), \quad (11)$$

where $\bar{\varphi}_\pi$ is the azimuthal angle of the pion. The determination of $a(\bar{\theta}_{N^*})$ from the observed pion angular distribution will be discussed in Sec. IX. For the present calculations, we will be interested in two special cases for both of which the double integral of Eq. (10) reduces to a simple expression.

We will first assume that the distribution of N^* is isotropic in the c.m.s. In this case, G_π is given by

$$G_\pi=1/(\bar{E}_{\pi,\max}-\bar{E}_{\pi,\min}), \quad (\bar{E}_{\pi,\min}<\bar{E}_\pi<\bar{E}_{\pi,\max}), \quad (12)$$

$$G_\pi=0, \quad (\bar{E}_\pi<\bar{E}_{\pi,\min} \text{ and } \bar{E}_\pi>\bar{E}_{\pi,\max}), \quad (12a)$$

where $\bar{E}_{\pi,\min}$ and $\bar{E}_{\pi,\max}$ are the minimum and maximum values of the total energy $\bar{E}_\pi$ of the pion emitted in the decay of m_1. $\bar{E}_{\pi,\min}$ and $\bar{E}_{\pi,\max}$ are given by

$$\begin{aligned}\bar{E}_{\pi,\max}&=\bar{\gamma}_1(E_\pi^*+\bar{v}_1p_\pi^*),\\ \bar{E}_{\pi,\min}&=\bar{\gamma}_1(E_\pi^*-\bar{v}_1p_\pi^*),\end{aligned} \quad (13)$$

where E_π^* and p_π^* are the total energy and momentum of the pion in the rest system of m_1, $\bar{v}_1$ is the c.m.s. velocity of m_1 (which depends on $\bar{E}$ and m_2), and $\bar{\gamma}_1\equiv(1-\bar{v}_1^2)^{-\frac{1}{2}}$. It may be noted that Eq. (12) gives a uniform distribution of energies between $\bar{E}_{\pi,\min}$ and $\bar{E}_{\pi,\max}$, and is normalized to 1:

$$\int_{\bar{E}_{\pi,\min}}^{\bar{E}_{\pi,\max}} G_\pi d\bar{E}_\pi=1. \quad (14)$$

The uniform distribution of pion energies is easily derived from the equation for $\bar{E}_\pi$:

$$\bar{E}_\pi=\bar{\gamma}_1(E_\pi^*+\bar{v}_1p_\pi^*\cos\theta_\pi^*), \quad (15)$$

[18] We note that the choice of the upper limit M_b for the integral of Eq. (9a) for N has no practical effect on the predictions of the present model. Thus a change of the upper limit of this integral, which would change its value, would merely lead to a readjustment of the value of k which gives the best fit to the observed multiplicity (Fig. 9), since the experimental data determine only the product kN [Eq. (54)].

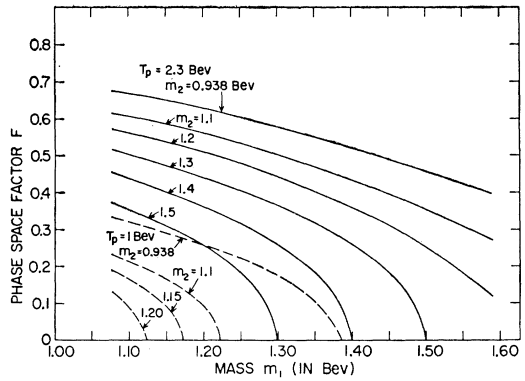

FIG. 1. Phase space factor F for single and double N^* production at proton energies $T_p=1.0$ and 2.3 Bev. The ordinate gives the values of $F=\bar{p}_1^2 d\bar{p}_1/d\bar{E}$ in units (Bev)$^2/c^3$. The full curves pertain to $T_p=2.3$ Bev; the dashed curves correspond to $T_p=1.0$ Bev.

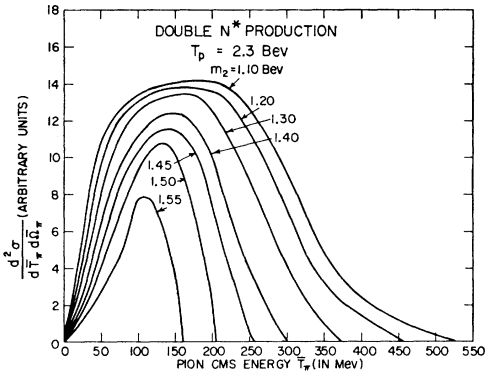

FIG. 2. Partial energy distributions for double pion production at a proton energy $T_p=2.3$ Bev for isotropic production of N^* in the c.m.s. The function shown in this figure is

$$\int_{M_a}^{M_{1,s}} \sigma(m_1) F G_\pi dm_1,$$

where m_1 is the mass of the decaying isobar N_1^*. The different curves pertain to various values of the mass m_2 of the other isobar N_2^* produced in the collision.

where θ_π^* is the angle of emission of the pion in the m_1-rest system. The number of decays per unit energy interval $d\bar{E}_\pi$ is given by

$$G_\pi=\frac{dn}{d\bar{E}_\pi}=\frac{dn}{d\cos\theta_\pi^*}\frac{d\cos\theta_\pi^*}{d\bar{E}_\pi}. \tag{16}$$

It is assumed throughout the present work that the isobar decays isotropically in its rest system.[19] Thus $dn/d\cos\theta_\pi^*$ is constant ($=\frac{1}{2}$). In view of Eq. (15), we have

$$d\cos\theta_\pi^*/d\bar{E}_\pi=1/(\bar{\gamma}_1\bar{v}_1\bar{p}_\pi^*), \tag{17}$$

which is also independent of θ_π^*. This shows that $dn/d\bar{E}_\pi=G_\pi$ is constant between the limits $\bar{E}_{\pi,\min}$ and $\bar{E}_{\pi,\max}$.

The procedure of the calculation of $d^2\sigma/d\bar{T}_\pi d\bar{\Omega}_\pi$ from Eq. (9) was as follows. The phase space factor F was calculated for $m_2=0.938$ Bev (single production) and for various values of m_2 between 1.10 and 1.55 Bev (double production). The curves of F *vs* m_1 are shown in Fig. 1, for values of the incident proton kinetic energy in the laboratory system $T_p=1.0$ and 2.3 Bev. It is seen that F is slowly decreasing with increasing m_1, except near the upper limit M_1 in those cases in which $M_1=\bar{E}-m_2$, so that F becomes zero at $m_1=M_1$. Thus the factor F will have a relatively minor influence on the energy spectrum of the pions, except for the values of m_1 in the neighborhood of $\bar{E}-m_2$.

Between $m_2=1.10$ and 1.55 Bev, F was calculated at intervals of m_2 of 50 Mev. For each selected value of m_2, to be called m_{2j}, the following quantity was obtained for various m_1 at intervals of 25 Mev:

$$g_{ij}\equiv\sigma(m_{1i})F_{ij}/(\bar{T}_{\pi,\max}{}^{(ij)}-\bar{T}_{\pi,\min}{}^{(ij)}), \tag{18}$$

where m_{1i} is one of the selected values of m_1; F_{ij}, $\bar{T}_{\pi,\max}{}^{(ij)}$, and $\bar{T}_{\pi,\min}{}^{(ij)}$ are the values of F, $\bar{T}_{\pi,\max}$ and $\bar{T}_{\pi,\min}$ pertaining to m_{1i} and m_{2j}. Here $\bar{T}_{\pi,\max}$ and $\bar{T}_{\pi,\min}$ are the kinetic energies corresponding to $\bar{E}_{\pi,\max}$ and $\bar{E}_{\pi,\min}$, respectively [see Eq. (13)]. Equation (18) gives a step function of magnitude g_{ij} extending from $\bar{T}_{\pi,\min}{}^{(ij)}$ to $\bar{T}_{\pi,\max}{}^{(ij)}$ for each set of values m_{1i}, m_{2j}. The step functions g_{ij} for all of the m_1 were added together and a smooth curve was drawn through the sum. The resulting spectrum, to be called I_j, is a function only of $\bar{T}_\pi$ and m_{2j}. Thus

$$I_j(\bar{T}_\pi,m_{2j})=(\textstyle\sum_i g_{ij})\Delta m, \tag{19}$$

where $\Delta m=25$ Mev. For $m_2=m_p$, I_j is equal to the single integral in the second term of Eq. (9) and gives the shape of the pion spectrum for single production. $I_j(\bar{T}_\pi,m_p)$ will be called $I_{\pi,s}$.

For $m_{2j}>m_p+m_\pi$, $I_j(\bar{T}_\pi,m_{2j})$ gives the partial pion energy distribution for a fixed value of m_2 contributing to double production. Some of the curves of I_j obtained for $T_p=2.3$ Bev are shown in Fig. 2. In order to evaluate the double integral of the first term of (9) which gives the complete spectrum, the values of $I_j(\bar{T}_\pi,m_2)$ for neighboring values of m_2: m_{2j} and $m_{2,j+1}$ (differing by 50 Mev) were interpolated so as to obtain $I_j(\bar{T}_\pi,m_2)$ for $m_2=\frac{1}{2}(m_{2j}+m_{2,j+1})$. Thus values of $I_j(\bar{T}_\pi,m_2)$ at intervals of 25 Mev were available. The double integral of Eq. (9) was then obtained by multiplying by $\sigma(m_{2j})$ and summing over m_{2j}. We define

$$I_{\pi,d}(\bar{T}_\pi)\equiv\textstyle\sum_j I_j(\bar{T}_\pi,m_{2j})\sigma(m_{2j})\Delta m, \tag{20}$$

[19] From the interpretation of the pion scattering experiments,[13] it is known that the isobar has spin $J=\frac{3}{2}$. This value was also predicted from the strong coupling theory,[12] according to which the isobar has $T'=J=\frac{3}{2}$. Thus it is possible that the N^* will be partially polarized, in the same manner as protons which have been elastically scattered. Since the average spin direction would then be perpendicular to the plane of production, the pion would be emitted preferentially at a small angle to the plane of production. However, since J is not large, one expects that these effects will not be very important. For this reason and because of the lack of information about the polarization, we have used the assumption of isotropic decay.

where the values of m_2 cover the range from M_a to M_2. A smooth curve drawn through the values of $I_{\pi,d}$ from Eq. (20) gives the shape of the pion spectrum for double production.

The preceding calculations were carried out for incident proton kinetic energies $T_p=0.8$, 1.0, 1.5, 2.3, and 3.0 Bev. Figure 3 shows the shape of the pion spectrum $I_{\pi,s}$ for single production. $I_{\pi,s}$ is given by

$$I_{\pi,s}=\int_{M_a}^{M_{1,s}}\sigma(m_1)FG_\pi dm_1. \tag{21}$$

It is seen that the maxima of $I_{\pi,s}(\bar{T}_\pi)$ are quite broad. For $T_p\gtrsim 1.5$ Bev, the maximum extends to considerably higher energies than the maximum of the cross section $\sigma(m_1)$ which would give a rather narrow peak at $\bar{T}_\pi=120$ Mev for an excited nucleon decaying at rest in the c.m.s. The broadening of the maximum is due to the motion of the excited nucleons, which becomes an important effect with increasing proton energy.

Figure 4 shows values of $I_{\pi,d}$:

$$I_{\pi,d}=\int_{M_a}^{M_2}dm_2\int_{M_a}^{M_{1,d}}\sigma(m_1)\sigma(m_2)FG_\pi dm_1, \tag{22}$$

giving the pion spectrum for double pion production, for $T_p=1.0$, 1.5, 2.3, and 3.0 Bev. At 1.0 Bev, double production is almost negligible, due to the smallness of the phase space factor. A comparison of Fig. 4 with Fig. 3 shows that the maximum of the $I_{\pi,d}$ curves is somewhat narrower than that of $I_{\pi,s}$. Thus for $T_p=2.3$ Bev, the full width at half maximum is 240 Mev for double production (from $\bar{T}_\pi\cong 40$ to 280 Mev), as compared to 330 Mev for single production (from $\bar{T}_\pi\cong 25$ to 355 Mev). Similarly for $T_p=3.0$ Bev, the half-maximum width is 310 Mev for double production, as compared to 380 Mev for single production. This narrowing of the maximum arises from the additional factor $\sigma(m_2)$ in the integrand of $I_{\pi,d}$. This factor

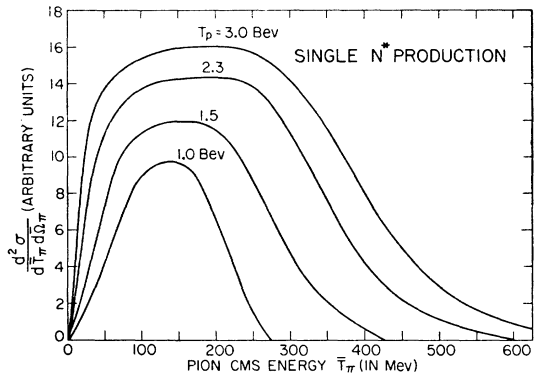

FIG. 3. Energy spectrum in the c.m.s. for single pion production at proton energies $T_p=1.0$, 1.5, 2.3, and 3.0 Bev for isotropic production of N^* in the c.m.s. The curves represent the single integral $I_{\pi,s}$ of Eq. (9).

makes it most probable that m_2 will have a value close to the resonance value of 1.22 Bev. For a fixed m_2, the momentum $\bar{p}_1$ of a given m_1 would be completely determined. This value of $\bar{p}_1$ will be smaller than that for single production (for which $m_2=m_p$). Therefore the spread $\Delta\bar{E}_\pi\equiv\bar{E}_{\pi,\max}-\bar{E}_{\pi,\min}$ of the pion energies will be reduced, since $\Delta\bar{E}_\pi$ is proportional to $\bar{p}_1$, being given by

$$\Delta\bar{E}_\pi=2\bar{p}_1p_\pi^*/m_1. \tag{23}$$

Figures 3 and 4 show that the broadening of the pion spectrum due to the motion of the isobar is an important effect, although it does not shift appreciably the position of the maximum which is still in the region of 100–200 Mev for $T_p<3$ Bev.

III. EFFECT OF THE ANGULAR DISTRIBUTION OF THE ISOBAR ON THE PION ENERGY SPECTRUM

In view of our lack of information about the angular distribution of the nucleon isobars produced in the

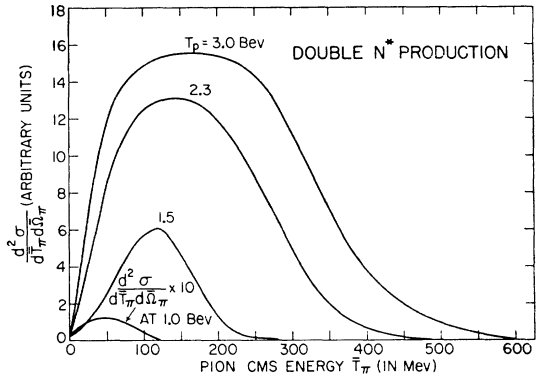

FIG. 4. Energy spectrum for double pion production at proton energies $T_p=1.0$, 1.5, 2.3, and 3.0 Bev for isotropic production of N^* in the c.m.s. The curves represent the double integral $I_{\pi,d}$ of Eq. (9). For 1.0 Bev, the double production is very small, and the values of $10I_{\pi,d}$ are shown in the figure.

nucleon-nucleon collision, it seems of interest to treat two extreme cases which differ markedly from the isotropic distribution considered above. We shall discuss the case where the N^* is made only in the forward and backward directions in the c.m.s. The pion spectrum will be calculated for the pions emitted in the forward direction and for the pions observed at 90° in the c.m.s. These spectra will be referred to as the 0° and 90° spectra, respectively.[20]

We will consider first the 0° spectrum. In general, the Jacobian J which enters into Eq. (10) for G_π is given by

$$J=\frac{\bar{\gamma}_1^2[1+(\rho^*)^2+2\rho^*\cos\theta_\pi^*-\bar{v}_1^2\sin^2\theta_\pi^*]^{\frac{3}{2}}}{1+\rho^*\cos\theta_\pi^*}, \tag{24}$$

[20] The same 0° and 90° spectra would also apply if the isobar N^* is made only at 90° c.m.s. angle to the incident proton direction. In this case, the 90° spectrum would give the energy distribution of the pions emitted in the forward direction, while the 0° spectrum would apply to the pions observed at 90° in the c.m.s.

where $\bar{v}_1$ is the velocity of the excited nucleon m_1, θ_π^* is the angle between the direction of the isobar and that of the pion in the m_1-rest system; $\rho^* \equiv \bar{v}_1/v_\pi^*$, where v_π^* is the velocity of the pion in the m_1-rest system. From Eq. (24), the values of J for $\theta_\pi^*=0°$ and 180° are given by

$$J_a=\bar{\gamma}_1^2(1+\rho^*)^2, \quad (\theta_\pi^*=0°) \tag{24a}$$

$$J_b=\bar{\gamma}_1^2(1-\rho^*)^2, \quad (\theta_\pi^*=180°). \tag{24b}$$

The pion is obviously emitted in the forward direction in the c.m.s. if the isobar is produced in the forward direction ($\bar{\theta}_{N^*}=0°$) and the decay angle θ_π^* is 0°. This case corresponds to Eq. (24a). If the isobar is produced in the backward direction and emits the pion at $\theta_\pi^*=180°$, the pion is observed along the forward direction in the c.m.s., provided that $v_\pi^*>\bar{v}_1$. However, when the available energy in the m_1-rest system, $m_1-(m_p+m_\pi)$, is very small, so that $v_\pi^*<\bar{v}_1$, the pion emitted at $\theta_\pi^*=180°$ travels in the same direction in the c.m.s. as the parent isobar, so that the latter must have been produced in the forward direction in order to contribute to the pion spectrum at 0°. For both of these possibilities for $\theta_\pi^*=180°$, the Jacobian is given by (24b). The values of $\bar{E}_\pi$ which correspond to J_a and J_b are $\bar{E}_{\pi,\max}$ and $\bar{E}_{\pi,\min}$, respectively, as given by Eq. (13). Thus the pion spectrum is obtained from Eq. (9), in which G_π is given by

$$G_\pi(\bar{E}_\pi)=\bar{\gamma}_1^2(1+\rho^*)^2\delta[\bar{E}_\pi-\bar{\gamma}_1(E_\pi^*+\bar{v}_1 p_\pi^*)] +\bar{\gamma}_1^2(1-\rho^*)^2\delta[\bar{E}_\pi-\bar{\gamma}_1(E_\pi^*-\bar{v}_1 p_\pi^*)]. \tag{25}$$

The δ functions in Eq. (25) correspond to the fact that for an isobar with a fixed mass m_1 emitting a pion at $\theta_\pi^*=0°$ or 180°, there is a single pion energy $\bar{E}_\pi$. These δ functions replace the continuous spectrum of Eq. (12) which is obtained when the isobar is produced isotropically in the c.m.s. In view of Eq. (25), the step function g_{ij} of Eq. (18) (pertaining to m_{1i}, m_{2j}) is replaced by a sum of two-step functions $g_{ij,a}$ and $g_{ij,b}$ which were obtained as follows:

$$g_{ij,a}\equiv\frac{\sigma(m_{1i})F_{ij}J_{ij,a}}{\bar{T}_{\pi,\max}{}^{(ij+)}-\bar{T}_{\pi,\max}{}^{(ij-)}}, \tag{26}$$

where

$$\bar{T}_{\pi,\max}{}^{(ij-)}\equiv\tfrac{1}{2}[\bar{T}_{\pi,\max}{}^{(i-1,j)}+\bar{T}_{\pi,\max}{}^{(ij)}], \tag{27}$$

$$\bar{T}_{\pi,\max}{}^{(ij+)}\equiv\tfrac{1}{2}[\bar{T}_{\pi,\max}{}^{(ij)}+\bar{T}_{\pi,\max}{}^{(i+1,j)}]. \tag{27a}$$

The step function $g_{ij,a}$ extends from $\bar{T}_{\pi,\max}{}^{(ij-)}$ to $\bar{T}_{\pi,\max}{}^{(ij+)}$ and represents the contribution of values of m_1 between $\frac{1}{2}(m_{1,i-1}+m_{1i})$ and $\frac{1}{2}(m_{1i}+m_{1,i+1})$. In Eq. (26), $J_{ij,a}$ is obtained from (24a).

The step function $g_{ij,b}$ for $\theta_\pi^*=180°$ is given by

$$g_{ij,b}\equiv\frac{\sigma(m_{1i})F_{ij}J_{ij,b}}{\bar{T}_{\pi,\min}{}^{(ij+)}-\bar{T}_{\pi,\min}{}^{(ij-)}}, \tag{28}$$

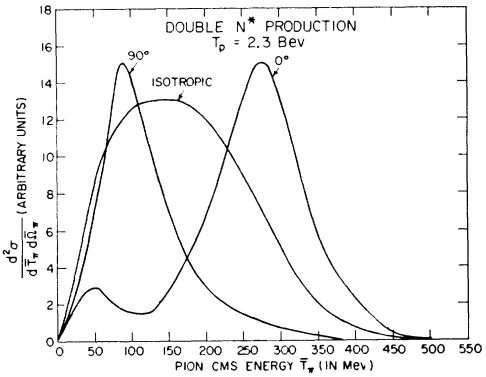

FIG. 5. A comparison of the energy spectra for double pion production at a proton energy $T_p=2.3$ Bev for isotropic and forward-backward emission of the isobars. The curves give the double integral $I_{\pi,d}$ of Eq. (9). The curve marked isotropic pertains to isotropic production of N^* in the c.m.s. The curves marked 0° and 90° were obtained on the assumption that N^* is made only in the forward and backward directions in the c.m.s. The 0° and 90° curves pertain, respectively, to the pions produced in the forward direction and at 90° in the c.m.s.

where $\bar{T}_{\pi,\min}{}^{(ij+)}$ and $\bar{T}_{\pi,\min}{}^{(ij-)}$ are defined in terms of $\bar{T}_{\pi,\min}{}^{(i\pm1,j)}$ and $\bar{T}_{\pi,\min}{}^{(ij)}$ in the same manner as in Eqs. (27) and (27a). $J_{ij,b}$ is obtained from (24b). The step function $g_{ij,b}$ extends from $\bar{T}_{\pi,\min}{}^{(ij-)}$ to $\bar{T}_{\pi,\min}{}^{(ij+)}$.

The spectra due to $g_{ij,a}$ and $g_{ij,b}$ must be added and summed over the m_{1i} in order to obtain the composite spectrum, $I_j(\bar{T}_\pi,m_{2j})$ [see Eq. (19)]. We note that, in contrast to the isotropic case, the step functions $g_{ij,a}$ (or $g_{ij,b}$) for different i do not overlap. Thus $g_{ij,a}$ is contiguous to $g_{i+1,j,a}$ (pertaining to $m_{1,i+1}$) generally on the high-energy side, and to $g_{i-1,j,a}$ (pertaining to $m_{1,i-1}$) on the low-energy side. The complete spectrum for double production is obtained from Eq. (19) in the same manner as for the isotropic case.

Figure 5 shows the 0° spectrum, together with the 90° spectrum and the energy distribution for the isotropic case, for double N^* production at $T_p=2.3$ Bev. The large peak of the 0° spectrum at 275 Mev is due to isobar decays with $\theta_\pi^*=0°$ for which the Jacobian, Eq. (24a), is generally $\gg1$. On the other hand, the weak maximum at 50 Mev is mainly due to pions emitted at $\theta_\pi^*=180°$. In this case, the N^* is generally moving backward in the c.m.s., and the corresponding Jacobian, given by Eq. (24b), is relatively small.

The 90° spectrum will now be obtained. For this purpose, the Jacobian (24) will be written in terms of the c.m.s. quantities:

$$J=\frac{(1-\bar{v}_1^2)}{(1+\bar{\rho}^2-2\bar{\rho}\cos\bar{\theta}_\pi-\bar{v}_1^2\sin^2\bar{\theta}_\pi)^{\frac{1}{2}}(1-\bar{\rho}\cos\bar{\theta}_\pi)}, \tag{29}$$

where $\bar{\theta}_\pi$ = c.m.s. angle between excited nucleon and pion, $\bar{\rho}\equiv\bar{v}_1/\bar{v}_\pi$, with $\bar{v}_\pi$ = velocity of pion in c.m.s. For $\bar{\theta}_\pi=90°$, Eq. (29) gives

$$J=(1-\bar{v}_1^2)/(1+\bar{\rho}^2-\bar{v}_1^2)^{\frac{1}{2}}. \tag{29a}$$

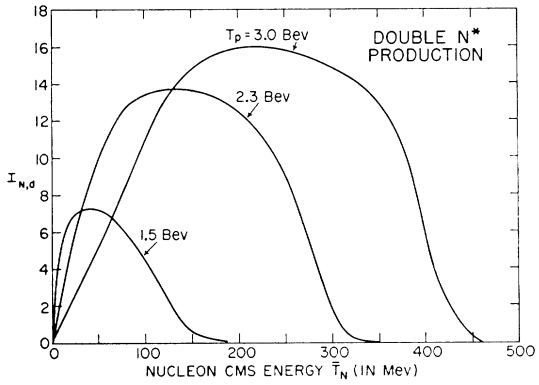

FIG. 6. Energy spectrum of the recoil nucleons $I_{N,d}$ for double N^* production at incident proton energies $T_p=1.5$, 2.3, and 3.0 Bev for isotropic production of N^* in the c.m.s. These curves have the same normalization as $I_{\pi,d}$ in Fig. 4.

The pion energy $\bar{E}_\pi$ is $E_\pi^*/\bar{\gamma}_1$, so that

$$G_\pi(\bar{E}_\pi)=\frac{1-\bar{v}_1^2}{(1+\bar{\rho}^2-\bar{v}_1^2)^{\frac{1}{2}}}\delta\left(\bar{E}_\pi-\frac{E_\pi^*}{\bar{\gamma}_1}\right). \tag{30}$$

Hence g_{ij} becomes

$$g_{ij}=\sigma(m_{1i})F_{ij}J_{ij}/(\bar{T}_\pi^{(ij+)}-\bar{T}_\pi^{(ij-)}), \tag{31}$$

where

$$\bar{T}_\pi^{(ij\pm)}\equiv\tfrac{1}{2}[\bar{T}_\pi^{(i\pm1,j)}+\bar{T}_\pi^{(ij)}]. \tag{32}$$

The step function g_{ij} extends from $\bar{T}_\pi^{(ij-)}$ to $\bar{T}_\pi^{(ij+)}$. In Eq. (31), J_{ij} is obtained from (29a) and $\bar{T}_\pi^{(ij)}$ is given by $(E_\pi^*/\bar{\gamma}_1)-m_\pi$. The resulting spectrum for double pion production at $T_p=2.3$ Bev is shown in Fig. 5. It is seen that the maximum of $d^2\sigma/d\bar{T}_\pi d\bar{\Omega}_\pi$ is narrower and occurs at a lower energy than for the isotropic distribution. This was to be expected, since the pion energy is $E_\pi^*/\bar{\gamma}_1$ for the 90° spectrum, which is smaller by a factor $\bar{\gamma}_1^2$ than the average energy $\bar{\gamma}_1 E_\pi^*$ for the isotropic case.

IV. ENERGY SPECTRUM OF RECOIL NUCLEONS

The energy spectrum of the recoil nucleons is obtained from the following equation, similar to Eq. (9) for the pions:

$$\frac{d^2\sigma}{d\bar{T}_N d\bar{\Omega}_N}=A\left[\int_{M_a}^{M_2}dm_2\int_{M_a}^{M_{1,d}}\sigma(m_1)\sigma(m_2)FG_{N,1}dm_1+kN\int_{M_a}^{M_{1,s}}\sigma(m_1)F(G_{N,1}+G_{N,2})dm_1\right]. \tag{33}$$

Here $d^2\sigma/d\bar{T}_N d\bar{\Omega}_N$ gives the number of events in which one of the recoil nucleons has kinetic energy between $\bar{T}_N$ and $\bar{T}_N+d\bar{T}_N$, and is emitted into the solid angle $d\bar{\Omega}_N$. For the calculations of this section, it will be assumed that the N^* is made isotropically in the c.m.s. $G_{N,1}$ is the energy distribution of the nucleons arising from the decay of N^* and is given by

$$G_{N,1}=1/(\bar{E}_{N,\max}-\bar{E}_{N,\min}),\quad(\bar{E}_{N,\min}<\bar{E}_N<\bar{E}_{N,\max}), \tag{34}$$

$$G_{N,1}=0,\quad(\bar{E}_N<\bar{E}_{N,\min}\text{ and }\bar{E}_N>\bar{E}_{N,\max}), \tag{34a}$$

where $\bar{E}_N$ is the total energy of the nucleon in the c.m.s., and

$$\bar{E}_{N,\max}=\bar{\gamma}_1(E_N^*+\bar{v}_1 p_N^*),\qquad \bar{E}_{N,\min}=\bar{\gamma}_1(E_N^*-\bar{v}_1 p_N^*), \tag{35}$$

with E_N^* = total energy, p_N^* = momentum of the nucleon in the rest system of the isobar of mass m_1.

The term $G_{N,2}$ in the single integral of (33) pertains to the unexcited nucleon in the reaction $p+p\rightarrow N^*+(p \text{ or } n)$. We note that since the nucleon isobar has isotopic spin $T'=\frac{3}{2}$, it may exist in the doubly charged state, in which case a neutron will be made together with the N^*. $G_{N,2}$ is given by

$$G_{N,2}=\delta(\bar{E}_N-\bar{E}_{N,0}), \tag{36}$$

where $\bar{E}_{N,0}$ is the energy of the nucleon made directly. $\bar{E}_{N,0}$ depends on m_1 and on the total energy $\bar{E}$ in the c.m.s.

In order to obtain the energy spectrum of the recoil protons, we must consider the wave function for the final state, which is either N^*+N^* or N^*+N. For double N^* production, the total wave function Ψ for p-p collisions is

$$\Psi_{p-p}^{(2)}=-(3/10)^{\frac{1}{2}}\psi_{\frac{3}{2}}(1)\psi_{-\frac{1}{2}}(2)+(4/10)^{\frac{1}{2}}\psi_{\frac{1}{2}}(1)\psi_{\frac{1}{2}}(2)-(3/10)^{\frac{1}{2}}\psi_{-\frac{1}{2}}(1)\psi_{\frac{3}{2}}(2), \tag{37}$$

where $\psi_{Tz'}$ is the wave function for the isobaric state with $T'=\frac{3}{2}$ and z-component T_z' [charge $=e(T_z'+\frac{1}{2})$]. The number in parentheses (1) or (2) labels the two excited nucleons. For the decay of the isobar, the functions $\psi_{\frac{3}{2}}$, $\psi_{\frac{1}{2}}$, and $\psi_{-\frac{1}{2}}$ are equivalent to the following:

$$\psi_{\frac{3}{2}}=\mu_1\chi_{\frac{1}{2}}, \tag{38}$$

$$\psi_{\frac{1}{2}}=(\tfrac{2}{3})^{\frac{1}{2}}\mu_0\chi_{\frac{1}{2}}+(\tfrac{1}{3})^{\frac{1}{2}}\mu_1\chi_{-\frac{1}{2}}, \tag{39}$$

$$\psi_{-\frac{1}{2}}=(\tfrac{1}{3})^{\frac{1}{2}}\mu_{-1}\chi_{\frac{1}{2}}+(\tfrac{2}{3})^{\frac{1}{2}}\mu_0\chi_{-\frac{1}{2}}, \tag{40}$$

where μ_{t_z} is the pion wave function with isotopic spin t_z (e.g., μ_1 represents a π^+ meson); χ_{t_z} is the nucleon wave function ($\chi_{\frac{1}{2}}$ = proton, $\chi_{-\frac{1}{2}}$ = neutron). The probability distribution P obtained from (37) is

$$P=(6/10)\psi_{\frac{3}{2}}^2\psi_{-\frac{1}{2}}^2+(4/10)(\psi_{\frac{1}{2}}^2)^2. \tag{41}$$

The two terms of (41) will be called a and b, respectively. From (38) and (40), one obtains, for the number of protons due to a,

$$n_a=(6/10)(1+\tfrac{1}{3})=\tfrac{4}{5}. \tag{42}$$

Similarly, b gives

$$n_b=(4/10)(4/3)=8/15, \tag{42a}$$

so that the total number of protons is

$$n_a+n_b=4/3. \tag{43}$$

For single N^* production, Ψ is given by

$$\Psi_{p-p}{}^{(1)}=-\tfrac{1}{2}\psi_{\frac{1}{2}}\eta_{\frac{1}{2}}+\tfrac{1}{2}\sqrt{3}\psi_{\frac{1}{2}}\eta_{-\frac{1}{2}}, \tag{44}$$

where η_{t_z} is the wave function of the unexcited nucleon. Thus the fraction of unexcited protons is $\frac{1}{4}$. From Eqs. (37)–(39), the number of protons from the decay of the isobar is

$$n=(\tfrac{1}{4})(\tfrac{2}{3})+\tfrac{3}{4}=11/12. \tag{45}$$

In view of (33), (43), and (45), the energy spectrum of the recoil protons is given by

$$\frac{d^2\sigma(p)}{d\bar{T}_p d\bar{\Omega}_p}=A\{(4/3)I_{N,d}+kN[(11/12)I_{N,1}+\tfrac{1}{4}I_{N,2}]\}, \tag{46}$$

where $\bar{T}_p$ and $d\bar{\Omega}_p$ are the proton energy and solid angle, respectively; $I_{N,d}$ is the double integral of Eq. (33); $I_{N,1}$ and $I_{N,2}$ are defined by

$$I_{N,i}\equiv\int_{M_a}^{M_{1,s}}\sigma(m_1)FG_{N,i}dm_1. \tag{47}$$

We note that the corresponding expression for the neutron spectrum is

$$\frac{d^2\sigma(n)}{d\bar{T}_n d\bar{\Omega}_n}=A[\tfrac{2}{3}I_{N,d}+kN(\tfrac{1}{12}I_{N,1}+\tfrac{3}{4}I_{N,2})]. \tag{48}$$

The integrals $I_{N,d}$ and $I_{N,1}$ are evaluated in the same manner as the corresponding integrals $I_{\pi,d}$ and $I_{\pi,s}$ for the pion spectrum for isotropic production of the N^*. On the other hand, $I_{N,2}$ is similar to the pion integrals for the 0° or 90° spectrum, since $G_{N,2}$ is a delta function which is analogous to Eqs. (25) and (30).

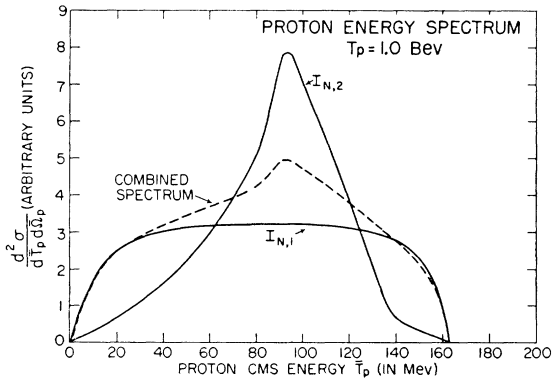

FIG. 7. Energy spectrum of the recoil protons at $T_p=1.0$ Bev. The combined spectrum is shown together with the components $I_{N,1}$ and $I_{N,2}$. $I_{N,1}$ corresponds to protons from the decay of N^*; $I_{N,2}$ pertains to protons which have not been excited in the collision. The combined spectrum is proportional to $[(11/12)I_{N,1}+(1/4)I_{N,2}]$.

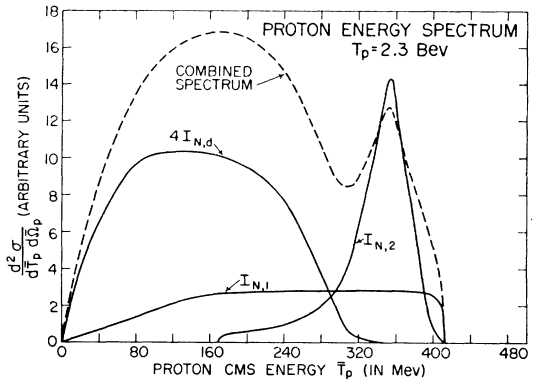

FIG. 8. Energy spectrum of the recoil protons at $T_p=2.3$ Bev. The combined spectrum is shown, together with the components $I_{N,d}$, $I_{N,1}$, and $I_{N,2}$. $I_{N,d}$ pertains to protons arising from double N^* production; $I_{N,1}$ and $I_{N,2}$ correspond to single N^* production. The combined spectrum is proportional to

$$\{(4/3)I_{N,d}+0.6N[(11/12)I_{N,1}+(1/4)I_{N,2}]\}.$$

(The curve of $I_{N,d}$ does not have the same normalization as in Fig. 6.)

Figure 6 shows the values of the double integral $I_{N,d}$ of Eq. (33) giving the nucleon spectrum for double N^* production at $T_p=1.5$, 2.3, and 3.0 Bev. These curves have the same normalization as the curves of the pion spectra in Fig. 4. Thus

$$\int_0^{\bar{T}_{N,m}} I_{N,d}d\bar{T}_N=\int_0^{\bar{T}_{\pi,m}} I_{\pi,d}d\bar{T}_\pi, \tag{49}$$

where $\bar{T}_{N,m}$ is the maximum possible value of $\bar{T}_N$, above which $I_{N,d}=0$ in the present model, and $\bar{T}_{\pi,m}$ is the corresponding energy for the pion spectrum.

Figures 7 and 8 show the proton spectra for $T_p=1.0$ and 2.3 Bev. At 1.0 Bev, double N^* production is negligible. Figure 7 shows the functions $I_{N,1}$ and $I_{N,2}$ together with the combined spectrum as obtained from (46). It is seen that $I_{N,1}$ (protons from N^* decay) is quite flat over most of the energy range, whereas $I_{N,2}$ (unexcited protons) has a pronounced maximum near $\bar{T}_p=90$ Mev. The reason is that $I_{N,2}$ essentially reproduces the shape of the scattering cross section $\sigma(m_1)$, since to each value of m_1 there corresponds a unique proton energy $\bar{E}_{N,0}$. On the other hand, for the protons arising from the N^* decay, there is a range of energies $\bar{E}_N$ for each m_1, which accounts for the flat central part of the $I_{N,1}$ curve. It may be noted that the combined spectrum has only a weak maximum at 90 Mev, because of the relatively small coefficient of $I_{N,2}$ as compared to the coefficient of $I_{N,1}$, in (46).

Figure 8 shows the three spectral shapes $I_{N,d}$, $I_{N,1}$, and $I_{N,2}$ for $T_p=2.3$ Bev, together with the combined spectrum obtained with $k=0.6$. This value of k is derived in the next section from the comparison of the calculations with the experimental values of the pion multiplicity as a function of the incident proton energy.

At 2.3 Bev, the double production is very prominent and essentially determines the shape of the combined spectrum for $\bar{T}_p \lesssim 280$ Mev. However, $I_{N,d}$ becomes very small above 300 Mev, and, in this region, the proton spectrum is determined primarily by the single production. In similarity to the 1.0-Bev spectrum, $I_{N,1}$ is approximately constant over most of the range, whereas $I_{N,2}$ has a sharp maximum corresponding to the resonance of $\sigma(m_1)$. Figure 8 shows that the combined spectrum has two maxima, one in the range 100–200 Mev corresponding to the maximum for the double production $I_{N,d}$, and a second maximum near 350 Mev arising from the peak of $I_{N,2}$. It would therefore be of interest to make accurate measurements of the recoil proton spectrum in the region of $T_p \sim 2$ Bev, in order to determine whether these features are present. In the following section, we shall compare the calculated spectra of the recoil nucleons with the cloud chamber results[7] obtained at the Cosmotron.

V. COMPARISON OF CALCULATED PION AND NUCLEON ENERGY SPECTRA WITH EXPERIMENT

In the discussion given above (Secs. II and IV), we have obtained separately the pion and nucleon spectra due to single and double production. In order to obtain the combined spectra due to both processes it is necessary to determine the constant k of Eqs. (9) and (33). This will be done by comparing the calculated pion multiplicity with the experimental results obtained from the Brookhaven cloud-chamber data[7] and from the counter measurements of Lindenbaum and Yuan.[3]

In terms of the integrals $I_{\pi,d}$ and $I_{\pi,s}$ defined above, the differential cross section for pion production can be written

$$d^2\sigma/d\bar{T}_\pi d\bar{\Omega}_\pi = A(I_{\pi,d}+kNI_{\pi,s}). \tag{50}$$

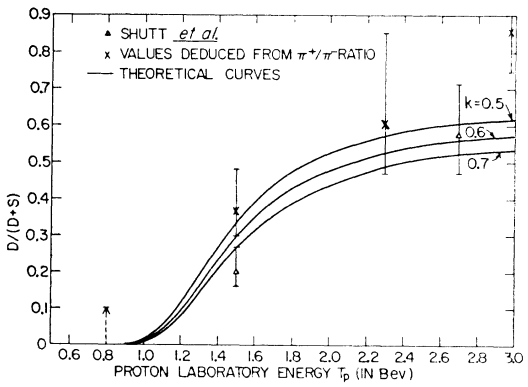

FIG. 9. Calculated and experimental values of the ratio of the cross section for producing two pions (D) to the sum of the cross sections for single and double production ($S+D$) in p-p collisions ($T=1$). The calculated curves were obtained from Eq. (54) with $k=0.5$, 0.6, and 0.7. The triangles represent the Brookhaven cloud-chamber results.[7] The crosses give the values of $D/(D+S)$ deduced from the π^+/π^- ratios measured by Lindenbaum and Yuan.[3]

We define

$$K_d \equiv \int_0^{\bar{T}_{\pi,m}} I_{\pi,d} d\bar{T}_\pi, \tag{51}$$

$$K_s \equiv \int_0^{\bar{T}_{\pi,m}} I_{\pi,s} d\bar{T}_\pi, \tag{51a}$$

where $I_{\pi,d}$ and $I_{\pi,s}$ are the energy spectra assuming isotropic distribution of the N^* in the c.m.s., as given in Figs. 3 and 4, and $\bar{T}_{\pi,m}$ is the maximum possible energy $\bar{T}_\pi$ above which $I_{\pi,d}$ or $I_{\pi,s}=0$. The total cross section for pion production σ_t becomes

$$\sigma_t = 4\pi A(K_d+kNK_s). \tag{52}$$

It should, however, be noted that the values of K_d and K_s are independent of the angular distribution of the N^*. Indeed, K_d and K_s, as given by Eqs. (51) and (51a), are equal to

$$K_d = \int_{M_a}^{M_2} dm_2 \int_{M_a}^{M_{1,d}} \sigma(m_1)\sigma(m_2)F dm_1, \tag{53}$$

$$K_s = \int_{M_a}^{M_{1,s}} \sigma(m_1)F dm_1. \tag{53a}$$

The equivalence of (53) and (51), and of (53a) and (51a) follows directly from the fact that the function G_π giving the energy distribution of the pions [see Eq. (9)] is normalized to 1, as shown by Eq. (14). The definition of K_d and K_s in terms of $I_{\pi,d}$ and $I_{\pi,s}$ is merely convenient here, since the functions $I_{\pi,d}$ and $I_{\pi,s}$ have been plotted in Figs. 3 and 4, whereas the integrals of Eqs. (53) and (53a) cannot be obtained directly from any results given in this paper.

The part of σ_t which is due to double production will be called D; the corresponding part for single production will be called S. The ratio of double to the sum of single plus double production events is thus given by

$$D/(D+S) = K_d/(K_d+kNK_s). \tag{54}$$

The ratio $D/(D+S)$ was obtained by Fowler *et al.* [reference 7(II)] at 1.5 Bev and by Block *et al.* [reference 7(III)] at 2.75 Bev. It was found that reasonable agreement with these data can be obtained by taking $k=0.6$. Figure 9 shows the curves of $D/(D+S)$ for $k=0.5$, 0.6, and 0.7, as obtained from Eq. (54). The Brookhaven cloud chamber results[7] are represented by the triangles. In addition, we have shown estimates of $D/(D+S)$ based on the measurements of the π^+/π^- ratio by Lindenbaum and Yuan.[3] It can be concluded that with the choice $k=0.6$, the present model gives reasonable agreement with the observed values of $D/(D+S)$ throughout the range from 1 to 3 Bev. It should be noted that at 3 Bev, there are some 3-pion events [reference 7(III)] ($\sim 15\%$ of the total inelastic cross section).

These events were not included in the comparison

since the present treatment of pion production via the $T'=J=\frac{3}{2}$ isobaric state only allows at most double pion production in a nucleon-nucleon collision. Hence the triple pion events would require other isobaric states involving double or triple meson decay. These states could in general have various other values of T' and J. Since we do not at present know the properties or even necessity of the existence of such states, they were not considered.

However, in principle one can conceive of meson production as always proceeding through a set of isobaric nucleon states of various T' and J values which decay by emitting one or more pions. Another possibility is that in addition to nucleon isobars, some pions are also produced directly.

In obtaining the combined π^+ spectrum due to single and double production, we will use $k=0.6$. The cross section for producing π^+ in p-p collisions is then given by

$$\frac{d^2\sigma(\pi^+)}{d\bar{T}_\pi d\bar{\Omega}_\pi}=A[(13/15)I_{\pi,d}+(0.6)(\tfrac{5}{6})NI_{\pi,s}], \quad (55)$$

where the coefficients 13/15 and 5/6 are obtained from Eqs. (37) and (44). Concerning the normalization constant N [see Eq. (9a)], it may be noted that with the (arbitrary) units used in Figs. 3 and 4, this constant becomes unity, so that the combined pion spectrum is obtained by adding $(13/15)I_{\pi,d}$ and $(1/2)I_{\pi,s}$, with $I_{\pi,d}$ and $I_{\pi,s}$ as given in Figs. 3 and 4. The resulting spectrum is shown in Fig. 10 for $T_p=1.0$ and 2.3 Bev, both for the isotropic distribution of N^* (full curves) and for the 90° case, i.e., on the assumption that N^* is made only in the forward and backward directions in the c.m.s., and the π^+ is observed at 90° in this system

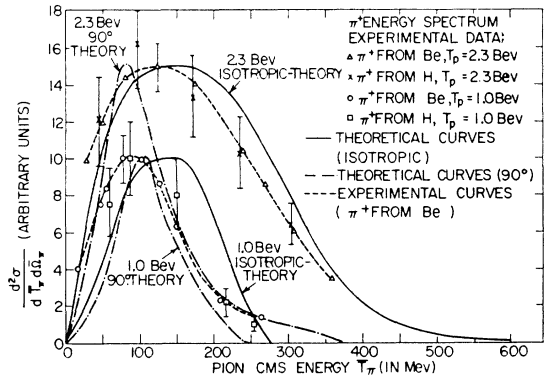

FIG. 10. Energy spectrum of π^+ mesons at $T_p=1.0$ and 2.3 Bev, as obtained from Eq. (9) with $k=0.6$. The solid curves pertain to isotropic production of N^* in the c.m.s. The dot-dashed curves correspond to production of N^* in the forward and backward directions and give the spectrum of π^+ mesons emitted at 90° in the c.m.s. The dashed curves show the results of Lindenbaum and Yuan[3] for 1.0 and 2.3-Bev protons on beryllium. Their data for hydrogen are also shown. The experimental and theoretical curves were normalized to the same value at the maximum of the cross section. The relative magnitude of these maxima at 1.0 and 2.3 Bev has no physical significance.

(dot-dashed curves in Fig. 10). These calculated values have been compared with the results of Lindenbaum and Yuan[3] for π^+ produced both in H and in Be. The experimental data have been normalized to the theoretical values at the maximum of the energy distribution. It may be noted that the experiments were carried out at a laboratory angle of 32° which corresponds to a range of c.m.s. angles from $\bar{\beta}_\pi\sim74°$ to $\sim100°$ at 2.3 Bev, and $\bar{\beta}_\pi\sim60°$ to 75° at 1.0 Bev. Figure 10 shows that for $T_p=2.3$ Bev the experimental spectrum follows closely the calculated curve for the isotropic case on the high-energy side of the maximum (at $\bar{T}_\pi\sim150$ Mev) thus giving an indication that the cross section for producing N^* is essentially isotropic in the c.m.s., which is also consistent with the cloud-chamber experiments [references 7(II), (III)]. Below ~125 Mev, the calculated results are somewhat too low. Aside from possible inadequacy of the theory, the discrepancy may be partly due to the experimental difficulties of obtaining accurate values of the pion intensity for low momenta mainly on account of the large positron and muon contamination. However, it is expected that more accurate values of the spectrum in this energy region will soon be available from experiments now being carried out by Lindenbaum and Yuan.[3] In any case, the present model is in good agreement with the existence of the low-energy peak of the pion spectrum and the rapid falloff of the pion distribution above the energy of the maximum.

For $T_p=1.0$ Bev, there is also an indication that the calculated values are somewhat too small for $\bar{T}_\pi\lesssim100$ Mev. At higher energies, the curve obtained from the 90° spectrum follows closely the experimental points. This result suggests that the production cross section of N^* may be peaked forward and backward in the c.m.s. at $T_p=1.0$ Bev. A similar conclusion is obtained below (Sec. IX) from the c.m.s. angular distribution of the pions at $T_p=0.8$ Bev, as observed by Morris, Fowler, and Garrison [reference 7(I)].

The Fermi statistical theory has been previously compared with various experiments, and it was shown that it does not predict correctly the observed distribution of pion multiplicities. Thus it gives values of the multiplicity which are considerably too small in the range $T_p\sim1$ to 3 Bev. In the usual comparisons of the energy spectra calculated from the Fermi theory, a part of the disagreement with experiment arises from the fact that the statistical weight of the spectrum due to single production is relatively too large, as compared to the statistical weight of the spectrum for double production. The relative weights for single and double production depend on the interaction volume assumed, while the individual spectral shapes for single and double production are independent of the volume. In order to obtain a more critical test of the Fermi theory, which does not involve the prediction of the multiplicity, we have compared the experimental spectra of Lindenbaum and Yuan[3] at 1.0 and 2.3 Bev with those

which would be obtained from the Fermi theory if one were to use the experimental values of the multiplicity.

At 1.0 Bev, the counter data[3] and the cloud chamber results[7] obtained at the Cosmotron show that there is essentially no double production. At 2.3 Bev, there is both single and double production. The experiments of Lindenbaum and Yuan[3] were carried out both with a beryllium target and with a hydrogen target. In the the former case, one has a mixture of p-p and n-p collisions. For the p-p interaction, the numbers of double and single production events are approximately equal [see Fig. 9; $D/(D+S)\cong 0.5$]. The total inelastic cross section was found by Fowler *et al.* [reference 7(IV)] to be 26 mb, giving 13 mb each for single and double production in the $T=1$ state. For n-p collisions, the fraction of the $T=0$ cross section which corresponds to inelastic (double production) events has not been measured. However, this fraction has been estimated from the behavior of the total $T=0$ cross section as a function of energy. This estimate is described in Sec. VI.

The shapes of the Fermi theory spectra for 1.0 and 2.3 Bev, and the branching ratios for the various single and double pion events for p-p and n-p collisions, have been calculated by Yang and Christian.[4] Upon using these ratios and the previously discussed cross sections, one obtains the appropriate momentum spectra for π^+ mesons produced in H and Be at 2.3 Bev. At 1.0 Bev, the double production is negligible, so that the beryllium and hydrogen π^+ momentum spectra are the same.

Figure 11 shows the calculated spectra at 1.0 Bev for Be or H, and at 2.3 Bev for Be together with the experimental results of Lindenbaum and Yuan,[3] which were found to be similar for both Be and H. For the Fermi theory calculations at 2.3 Bev, only the results for Be are shown. The curve for H is similar, except for somewhat more of a high-energy tail, which would give an even greater disagreement with the experimental spectrum. At each energy, the theoretical and experimental spectra have been normalized to the same area. It is seen that the curves obtained from the statistical theory are in considerable disagreement with the experimental values. The energy of the maximum of the calculated curves is considerably too high, and the maximum is quite wide, in contrast to the narrow peak of the experimental curves. For 2.3 Bev, there is, in addition, a high-energy tail which is contrary to the observations. This tail is due to the contribution of the single production. Thus Fig. 11 shows clearly that the Fermi statistical theory fails to give agreement with experiment because the partial energy spectra, especially for single production, have their maxima at energies which are considerably too high. This source of disagreement exists in addition to the failure of the statistical model to predict the observed multiplicities.

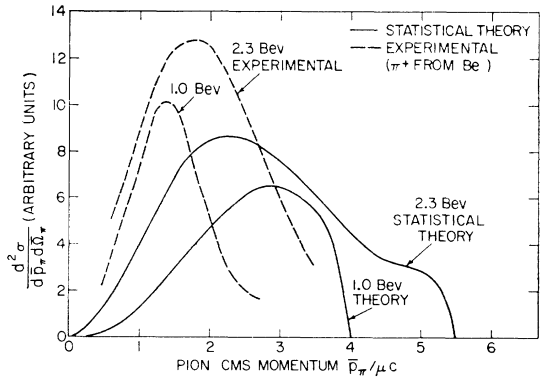

FIG. 11. Pion c.m.s. momentum spectra at 1.0 and 2.3 Bev as obtained from the Fermi statistical theory using the observed values of the pion multiplicity. The dashed curves give the experimental results of Lindenbaum and Yuan.[3]

We have also compared our results with those obtained with the Brookhaven hydrogen diffusion cloud chamber.[7] The experiments for which we have made calculations are those performed at 0.8 Bev by Morris, Fowler, and Garrison [reference 7(I)] and those carried out at 1.5 Bev by Fowler, Shutt, Thorndike, and Whittemore [reference 7(II)].

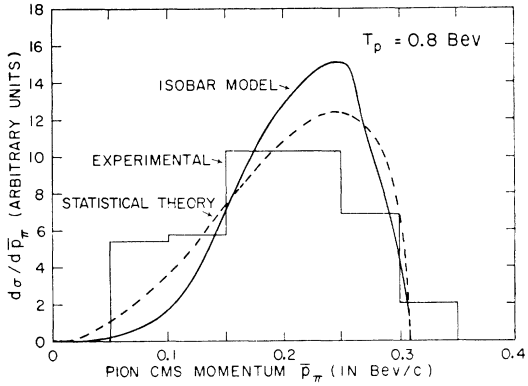

FIG. 12. Pion c.m.s. momentum spectrum at $T_p=0.8$ Bev. The solid curve was obtained from the isobar model [Eq. (56)]. The histogram represents the experimental data on $pn\pi^+$ events of Morris, Fowler, and Garrison [reference 7(I)]. The dashed curve gives the prediction of the Fermi statistical theory, as obtained by Block.[21] The two calculated curves and the histogram are normalized to the same area.

At 0.8 Bev, there is only single pion production. Consequently, the spectrum is completely determined by the integral $I_{\pi,s}$ of Eq. (21). In Fig. 12, we have plotted the calculated momentum spectrum as a function of the c.m.s. pion momentum $\bar{p}_\pi$ together with the histogram of the experimental results [reference 7(I)]. The theoretical curves give the values of

$$\frac{d^2\sigma}{d\bar{p}_\pi d\bar{\Omega}_\pi}=\bar{v}_\pi\frac{d^2\sigma}{d\bar{T}_\pi d\bar{\Omega}_\pi}\propto \bar{v}_\pi I_{\pi,s}, \tag{56}$$

where $\bar{v}_\pi$ is the c.m.s. velocity of the pion. The experimental and theoretical spectra have been normalized to the same area. It is seen that the calculations are in reasonable agreement with the experimental data.

In Fig. 12, we have also shown the prediction of the Fermi statistical theory, as obtained by Block.[21] At 0.8 Bev, there is no marked difference between the isobar model prediction and the result of the statistical theory. The momentum spectrum given by the Fermi theory goes as $\bar{p}_\pi^2$ near $\bar{p}_\pi=0$, whereas the spectrum obtained from the isobar model is proportional to $\bar{p}_\pi^4$ for small momenta for an isobar at rest in the c.m.s., since $\sigma \propto \bar{p}_\pi^4$ near $\bar{p}_\pi=0$. Thus both spectra start with zero slope at $\bar{p}_\pi=0$, and increase rapidly with momentum. At 0.8 Bev, it is just possible to form an isobar with mass values extending up to the upper limit of the resonance region. (The center of the resonance corresponds to $m_1 \cong 1.22$ Bev, while the maximum possible m_1 is 1.30 Bev.) Thus the isobar model curve of $d\sigma/d\bar{p}_\pi$ will have its maximum fairly close to the maximum possible momentum. For an isobar at rest in the c.m.s., the maximum of the $d\sigma/d\bar{p}_\pi$ curve would occur at the momentum p_π^* of the pion in the rest system of $m_1=1.22$ Bev ($p_\pi^*=220$ Mev/c), whereas the cutoff corresponds to the momentum p_π^* in the rest system of $m_1=1.30$ Bev ($p_\pi^*=290$ Mev/c). These two values are quite close to one another. The actual momenta at the maximum and cutoff taking into account the isobar motion are 250 and 305 Mev/c, respectively, as shown by Fig. 12. The curve predicted by the statistical model also has its maximum near the cutoff, but for a different reason: the phase space increases as $\bar{p}_\pi^2$ up to a momentum $\bar{p}_\pi$ fairly close to the cutoff, when the momenta of the recoil nucleons begin to have an appreciable effect. Thus the theoretical curves for the two models do not differ appreciably at 0.8 Bev, and both agree reasonably well with the experimental histograms. Therefore, the 0.8-Bev spectrum cannot be used to discriminate between the two models of pion production. On the other hand, at 1.5 Bev, as shown below, the spectrum given by the statistical theory differs considerably from the experimental histogram, because it predicts too many high-energy pions. However the curve obtained from the isobar model is in reasonably good agreement, thus giving evidence in favor of the isobar model. The reason for the enhancement of lower momentum pions in the isobar model, at an incident energy of 1.5 Bev, is that isobars can now be formed well beyond the peak of the resonance region and hence higher momentum pions are discriminated against by the rapidly decreasing resonance cross section on the high-energy side of the peak.

Figure 13 shows the spectrum of the recoil protons and neutrons at 0.8 Bev. In obtaining the proton energy spectrum for comparison with the cloud chamber results, we note that the experimental data include only protons from $pn\pi^+$ events. The energy spectrum for these protons is somewhat different from Eq. (46) which also contains a contribution from $pp\pi^0$ events. From Eq. (44), one finds that the momentum distribution of protons from $pn\pi^+$ alone is given by

$$\frac{d^2\sigma(p)_{pn\pi^+}}{d\bar{p}_p d\bar{\Omega}_p}=\bar{v}_p\frac{d^2\sigma(p)_{pn\pi^+}}{d\bar{T}_p d\bar{\Omega}_p}\propto \bar{v}_p(\tfrac{3}{4}I_{N,1}+\tfrac{1}{12}I_{N,2}), \quad (57)$$

where $\bar{v}_p$ is the c.m.s. velocity of the proton, and $\bar{p}_p$ is the proton momentum. Equation (57) was used to obtain the calculated curve for protons of Fig. 13. For the neutron momentum spectrum, one obtains from (48),

$$\frac{d^2\sigma(n)}{d\bar{p}_n d\bar{\Omega}_n}=\bar{v}_n\frac{d^2\sigma(n)}{d\bar{T}_n d\bar{\Omega}_n}\propto \bar{v}_n(\tfrac{1}{12}I_{N,1}+\tfrac{3}{4}I_{N,2}), \quad (58)$$

where $\bar{v}_n$ is the c.m.s. velocity of the neutron. For both protons and neutrons, the experimental and theoretical spectra have been normalized to the same area. Figure 13 shows that the calculated curves for 0.8 Bev are in satisfactory agreement with experiment. We note that the experimental histogram for the neutrons is more sharply peaked than that for the protons. In agreement with this feature, the calculated curve for neutrons has a higher maximum than that for protons. This difference between the two calculated spectra is due to the larger contribution of $I_{N,2}$ to the neutron spectrum [$\frac{3}{4}I_{N,2}$ as compared to $\frac{1}{12}I_{N,2}$ for the protons]. The dot-dashed curve in Fig. 13 was obtained from the Fermi statistical theory.[21] It is seen that this curve is practically the same as the isobar model prediction for the protons. Since the pion spectrum is closely the same for the two models, it was to be expected that the nucleon spectra would also be very similar at 0.8 Bev, since the pion and nucleon spectra are correlated by conservation of energy and momentum

Figures 14 and 15 show the corresponding spectra for $T_p=1.5$ Bev. In this case, only the parts of the theo-

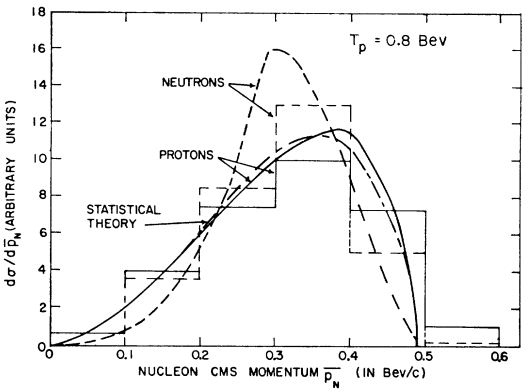

FIG. 13. c.m.s. momentum spectra of recoil protons and neutrons at $T_p=0.8$ Bev. The solid curve shows the proton spectrum obtained from the isobar model [Eq. (57)]; the dashed curve gives the calculated neutron spectrum [Eq. (58)]. The histograms represent the experimental data on $pn\pi^+$ events of Morris, Fowler, and Garrison [reference 7(I)] (solid lines for protons; dashed lines for neutrons). The dot-dashed curve gives the prediction of the Fermi statistical theory.[21] All of the curves and histograms are normalized to the same area.

[21] M. M. Block, Phys. Rev. **101**, 796 (1956).

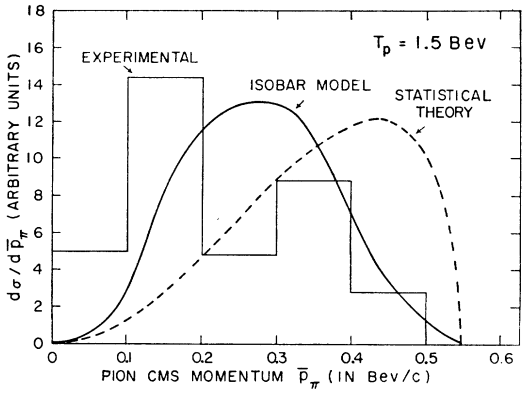

FIG. 14. Pion c.m.s. momentum spectrum at $T_p=1.5$ Bev. The solid curve was obtained from the isobar model [Eq. (56)]. The histogram represents the experimental data on $pn\pi^+$ events of Fowler, Shutt, Thorndike, and Whittemore [reference 7(II)]. The dashed curve gives the prediction of the Fermi statistical theory.[21] The two calculated curves and the histogram are normalized to the same area.

retical momentum distributions due to single production [Eqs. (56)–(58)] have been plotted, since the histograms of the experimental data represent only definite $pn\pi^+$ cases of single production [reference 7(II)]. For both pions and nucleons, the experimental and theoretical spectra have been normalized to the same area. It is seen that the spectra obtained from the isobar model are in satisfactory agreement with the experimental histograms. On the other hand, the results of the statistical theory[21] are in definite disagreement with experiment. The statistical theory gives too many high-energy pions and correspondingly the energy of the maximum of the nucleon spectrum is too low. Both deficiencies are remedied by the isobar model which favors the emission of low-energy pions and increases the relative number of high-energy recoil nucleons.[22]

VI. PION PRODUCTION IN n-p COLLISIONS

In the preceding discussion, we have considered only p-p interactions. The integrals of Eqs. (9) and (33) can also be used to obtain the energy spectra of pions and nucleons arising from n-p collisions. In this case, the initial system consists of an equal mixture of $T=0$ and $T=1$ states. For the production of one isobar, only the $T=1$ state contributes, since it is impossible to obtain a total angular momentum 0 with two component momenta of $\frac{3}{2}$ and $\frac{1}{2}$. However, for double N^* production, both the initial $T=0$ and $T=1$ states contribute.

[22] After the present calculations of the energy spectra were completed, it came to our attention that a similar calculation based on the model of an excited nucleon has been carried out by Yappa for the spectrum of pions produced by 600-Mev protons: Y. A. Yappa, quoted by Meshcheryakov, Zrelov, Neganov, Vzorov, and Shabudin, *Proceedings of the International Conference on the Peaceful Uses of Atomic Energy* (United Nations, New York, 1956), Vol. II. Belenkii and Nikishov have also considered the inclusion of isobars in the statistical theory: S. Z. Belenkii and A. I. Nikishov, J. Exptl. Theoret. Phys. (U.S.S.R.) **28**, 744 (1955) [translated in Soviet Phys. JETP **1**, 593 (1955)].

For single N^* production, the final state wave function is

$$\Psi_{n-p}{}^{(1)}=-(\tfrac{1}{2})^{\frac{1}{2}}\psi_{-\frac{1}{2}}\eta_{\frac{1}{2}}+(\tfrac{1}{2})^{\frac{1}{2}}\psi_{\frac{1}{2}}\eta_{-\frac{1}{2}}. \tag{59}$$

As in Eq. (44), ψ_{tz} denotes the wave function of the isobar, and η_{tz} is the wave function of the unexcited nucleon. From Eqs. (39), (40), and (59), one finds that the average numbers of the nucleons in the various final states are as follows: unexcited protons, $\frac{1}{2}$; protons from N^* decay, $\frac{1}{2}$; unexcited neutrons, $\frac{1}{2}$; neutrons from N^* decay, $\frac{1}{2}$. The fraction of pions in each charge state is, $n(\pi^+)=n(\pi^-)=\frac{1}{6}$; $n(\pi^0)=\frac{2}{3}$.

For double N^* production, the final state wave functions for $T=1$ and $T=0$ are given by

$$\begin{aligned}\Psi_{n-p}{}^{(2)}(T=1)&=(9/20)^{\frac{1}{2}}\psi_{\frac{3}{2}}(1)\psi_{-\frac{3}{2}}(2)-(1/20)^{\frac{1}{2}}\psi_{\frac{3}{2}}(1)\psi_{-\frac{1}{2}}(2)\\&\quad-(1/20)^{\frac{1}{2}}\psi_{-\frac{1}{2}}(1)\psi_{\frac{1}{2}}(2)+(9/20)^{\frac{1}{2}}\psi_{-\frac{3}{2}}(1)\psi_{\frac{3}{2}}(2),\end{aligned} \tag{60}$$

$$\begin{aligned}\Psi_{n-p}{}^{(2)}(T=0)&=-\tfrac{1}{2}\psi_{\frac{3}{2}}(1)\psi_{-\frac{3}{2}}(2)+\tfrac{1}{2}\psi_{\frac{3}{2}}(1)\psi_{-\frac{1}{2}}(2)\\&\quad-\tfrac{1}{2}\psi_{-\frac{1}{2}}(1)\psi_{\frac{1}{2}}(2)+\tfrac{1}{2}\psi_{-\frac{3}{2}}(1)\psi_{\frac{3}{2}}(2).\end{aligned} \tag{61}$$

The fractions of the various pion charge states are as follows: for $T=1$: $n(\pi^+)=n(\pi^-)=14/15$; $n(\pi^0)=2/15$; for $T=0$: $n(\pi^+)=n(\pi^0)=n(\pi^-)=\frac{2}{3}$. For both $T=1$ and $T=0$, one finds that, on the average, one proton and one neutron are made in the double N^* production case.

From the preceding results, one can obtain the spectra of pions and nucleons in n-p collisions. In the following, we will omit the normalization factor A for convenience [see Eqs. (46), (48), and (50)] and we will write simply σ_{n-p} for the spectral shape. One finds

$$\begin{aligned}\sigma_{n-p}(\pi^+)=\sigma_{n-p}(\pi^-)&=[(14/15)+\tfrac{2}{3}k_0]I_{\pi,d}\\&\quad+\tfrac{1}{6}kNI_{\pi,s},\end{aligned} \tag{62}$$

$$\sigma_{n-p}(\pi^0)=[(2/15)+\tfrac{2}{3}k_0]I_{\pi,d}+\tfrac{2}{3}kNI_{\pi,s}, \tag{63}$$

$$\begin{aligned}\sigma_{n-p}(p)=\sigma_{n-p}(n)&=I_{N,d}(1+k_0)\\&\quad+kN(\tfrac{1}{2}I_{N,1}+\tfrac{1}{2}I_{N,2}),\end{aligned} \tag{64}$$

where k_0 is the ratio of the total cross section for production of $2N^*$ in the $T=0$ state ($\sigma_{d,T=0}$) to the double production in the $T=1$ state. This ratio enters as an additional parameter for n-p collisions. The determination of $\sigma_{d,T=0}$ will be discussed below.

It may be convenient to list here the corresponding spectra for p-p collisions:

$$\sigma_{p-p}(\pi^+)=(13/15)I_{\pi,d}+(5/6)kNI_{\pi,s}, \tag{65}$$

$$\sigma_{p-p}(\pi^0)=(14/15)I_{\pi,d}+(1/6)kNI_{\pi,s}, \tag{66}$$

$$\sigma_{p-p}(\pi^-)=(3/15)I_{\pi,d}, \tag{67}$$

$$\sigma_{p-p}(p)=(4/3)I_{N,d}+kN[(11/12)I_{N,1}+\tfrac{1}{4}I_{N,2}], \tag{68}$$

$$\sigma_{p-p}(n)=\tfrac{2}{3}I_{N,d}+kN(\tfrac{1}{12}I_{N,1}+\tfrac{3}{4}I_{N,2}). \tag{69}$$

As an example of the difference between the energy spectra in n-p and p-p collisions, Fig. 16 shows the results obtained for an incident nucleon energy $T_N=1.5$ Bev. In this figure, we show two curves for the π^+

spectrum from p-p collisions and two curves for the $\pi^{\pm}$ spectrum from n-p collisions. It is evident that the spectra from n-p and p-p interactions will not differ appreciably when either single or double pion production predominates strongly, since in that case the shape of the spectrum is determined by $I_{\pi,s}$ or $I_{\pi,d}$ for single or double production, respectively. Significant differences between the n-p and p-p spectra can be expected only at intermediate energies such as 1.5 Bev, where the contributions of $I_{\pi,s}$ and $I_{\pi,d}$ are comparable, and differences arise because of the different coefficients of the I's for the n-p and p-p cases. The spectrum can be written

$$\sigma = c_d I_{\pi,d} + c_s I_{\pi,s}, \tag{70}$$

where c_d and c_s are the coefficients of $I_{\pi,d}$ and $I_{\pi,s}$, respectively, in Eqs. (62) and (65). The shape of the spectrum is determined by the ratio $\xi \equiv c_s/c_d$. For π^+ from p-p collisions, ξ is given by

$$\xi_{p-p}(\pi^+) = (5/6)k/(13/15) = 0.961k, \tag{71}$$

whereas for $\pi^{\pm}$ from n-p, one obtains

$$\xi_{n-p}(\pi^{\pm}) = \tfrac{1}{6}k/[(14/15) + \tfrac{2}{3}k_0] = k/(5.6+4k_0). \tag{72}$$

The curves for the π^+ spectra from p-p collisions in Fig. 16 were obtained using $k=0.6$ and 1.0, for which $\xi=0.576$ and 0.961, respectively. As has been shown above, the value $k=0.6$ gives the best fit to the observed pion multiplicity as a function of incident proton energy. However, the value of k is not known to better than ± 0.3, as a result of the experimental uncertainties. The curve for $k=1.0$ was calculated in order to show the sensitivity of the π^+ spectrum to the value of k. Since the single-pion energy distribution $I_{\pi,s}$ extends to higher energies than the double-pion spectrum $I_{\pi,d}$, it is evident that with increasing ξ, the spectrum falls off more slowly above the energy of the peak at $\bar{T}_\pi \cong 120$ Mev.

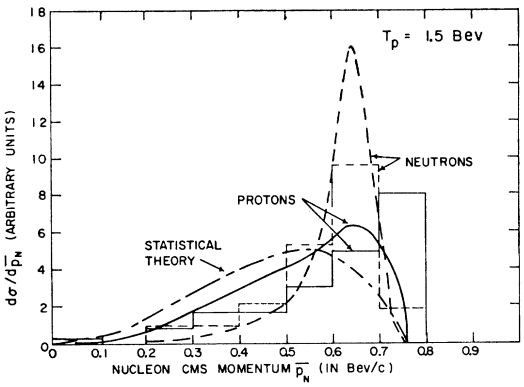

FIG. 15. c.m.s. momentum spectra of recoil protons and neutrons at $T_p=1.5$ Bev. The solid curve shows the proton spectrum obtained from the isobar model [Eq. (57)]; the dashed curve gives the calculated neutron spectrum [Eq. (58)]. The histograms represent the experimental data on $pn\pi^+$ events of Fowler, Shutt, Thorndike, and Whittemore [reference 7(II)] (solid lines: protons; dashed lines: neutrons). The dot-dashed curve gives the prediction of the Fermi statistical theory.[21] All of the curves and histograms are normalized to the same area.

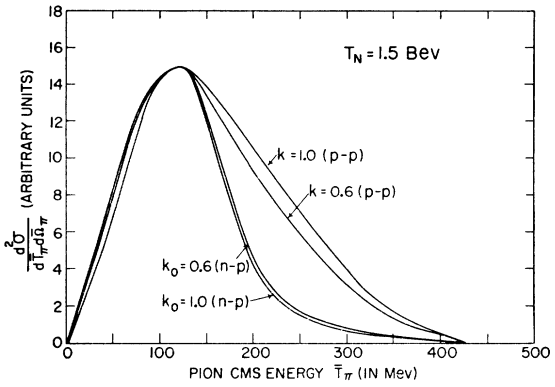

FIG. 16. Energy spectrum of pions from n-p and p-p collisions for an incident nucleon energy $T_N=1.5$ Bev. The two upper curves give the spectrum of π^+ mesons from p-p collisions, and were obtained from Eq. (62) with $k=0.6$ and 1.0. The two lower curves show the spectrum of $\pi^{\pm}$ mesons from n-p interactions, and were calculated from Eq. (65) with $k_0=0.6$ and 1.0; for both n-p cases, the value $k=0.6$ was used.

The two curves for $\pi^{\pm}$ production in n-p interactions in Fig. 16 were both obtained using $k=0.6$. If one assumes Eq. (83) below for the cross section $\sigma_{d,T=0}$ for production of $2N^*$ in the $T=0$ state, one obtains $k_0=1.1$ at 1.5 Bev. However, this value is subject to large uncertainties, as a result of our limited knowledge of $\sigma_{d,T=0}$, as is discussed below. The n-p curves of Fig. 16 were obtained using $k_0=0.6$ and 1.0. It is seen that these curves differ very little, showing that the spectrum is almost independent of the value of k_0. The corresponding values of ξ are very small. From (72) one finds $\xi=0.075$ and 0.0625 for $k_0=0.6$ and 1.0, respectively. Thus the spectral shape is approximately that for double N^* production, $I_{\pi,d}$. The reason is that for n-p collisions, a large fraction $(\frac{2}{3})$ of the single N^* production leads to the emission of π^0 mesons, with only $\frac{1}{6}$ of the cases giving π^+ and $\frac{1}{6}$ giving π^- mesons.

We have also compared our calculations with the results of the experiment by Fowler, Shutt, Thorndike, and Whittemore[6] on pion production by the forward (0°) neutron beam of the Cosmotron in the Brookhaven hydrogen diffusion cloud chamber. The neutron spectrum in this experiment extends from 1.0 to 2.2 Bev, the energy of the circulating proton beam. The largest group of double production events was the $pn\pi^+\pi^-$ group, i.e., cases in which both a π^+ and a π^- meson were emitted. The c.m.s. momentum spectrum of the pions for these cases has been obtained by the authors (see Fig. 21 of their paper[6]). We will now compare the results of the present isobar model with the observed $pn\pi^+\pi^-$ spectrum. From Eqs. (60) and (61), one obtains the following expression for the cross section for $pn\pi^+\pi^-$ events:

$$\sigma(pn\pi^+\pi^-) = \tfrac{1}{2}[(41/45)\sigma_{d,T=1} + (5/9)\sigma_{d,T=0}], \tag{73}$$

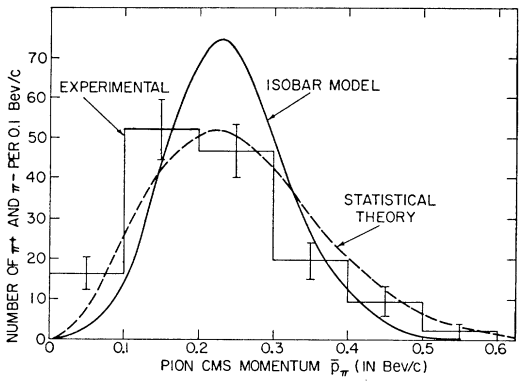

FIG. 17. c.m.s. momentum spectrum of pions from $pn\pi^+\pi^-$ events in n-p collisions obtained by Fowler, Shutt, Thorndike, and Whittemore[6] in the forward neutron beam of the Brookhaven Cosmotron at a proton energy of 2.2 Bev. The solid curve has been calculated from the present isobar model. The dashed curve was obtained by Fowler *et al.*[6] from the Fermi statistical theory.[4] The two theoretical curves are normalized to the number of observed events.

where $\sigma_{d,T=1}$ and $\sigma_{d,T=0}$ are the total cross sections for double production in the $T=1$ and $T=0$ states, respectively. The energy spectrum of the pions is given by

$$\langle I_{\pi,d}\rangle=\frac{\int_{1.0\text{ Bev}}^{2.2\text{ Bev}} I_{\pi,d}\sigma(pn\pi^+\pi^-)N(T_n)dT_n}{\int_{1.0\text{ Bev}}^{2.2\text{ Bev}} \sigma(pn\pi^+\pi^-)N(T_n)dT_n}, \quad (74)$$

where $N(T_n)dT_n$ is the number of incident neutrons in the energy interval between T_n and T_n+dT_n; $\langle I_{\pi,d}\rangle$ is the average of $I_{\pi,d}$ over the incident neutron spectrum. In order to obtain the values of $\sigma_{d,T=1}$ and $\sigma_{d,T=0}$ which enter in Eq. (73), we used the Brookhaven cloud-chamber results[7] and the counter data of Chen, Leavitt, and Shapiro.[23] From the cloud-chamber results, Fowler *et al.* [reference 7(IV)] have found that, between 1.0 and 3.0 Bev, the inelastic part of the $T=1$ cross section $\sigma_{\text{inel},T=1}$, remains approximately constant and has a value of 26 mb. Since triple production is negligible below 2.2 Bev, $\sigma_{\text{inel},T=1}$ represents only single and double production. Thus $\sigma_{d,T=1}$ is given by

$$\sigma_{d,T=1}=26[D/(D+S)]\text{ mb}, \quad (75)$$

where $D/(D+S)$ is the ratio of double to the sum of single plus double production. In the evaluation of (75) we used the theoretical curve of $D/(D+S)$ as obtained with $k=0.6$ (see Fig. 9), since this curve was shown to be in agreement with the experimental values of the multiplicity.

In order to obtain $\sigma_{d,T=0}$, we note that values of the $T=0$ cross section $\sigma_{T=0}$ have been deduced by Chen, Leavitt, and Shapiro[23] from their measurements of the cross section of protons on hydrogen and on deuterium. $\sigma_{T=0}$ remains approximately flat at 17–20 mb between 0.7 and 1.0 Bev. Above 1.0 Bev, $\sigma_{T=0}$ rises rapidly to a value of 36 mb at 1.6 Bev, and then becomes again approximately constant above 1.6 Bev. The rapid increase of $\sigma_{T=0}$ between 1.0 and 1.6 Bev has been interpreted as due to the onset of double pion production. As explained above, on the present isobar model, it is impossible to obtain single production in the $T=0$ state. We will therefore assume that the excess of $\sigma_{T=0}$ over the minimum value of 17 mb represents double pion production. On this assumption, the 17 mb would correspond to elastic scattering. Thus $\sigma_{d,T=0}$ was taken as

$$\sigma_{d,T=0}=\sigma_{T=0}-17\text{ mb}, \quad (76)$$

and the values of $\sigma_{T=0}$ were obtained from Table VIII of Chen, Leavitt, and Shapiro.[23]

The experimental neutron spectrum $N(T_n)$ is presented by Fowler *et al.*[6] as a histogram with intervals of 0.2 Bev ranging from 1.0 to 2.2 Bev. Correspondingly, the integrals in the numerator and denominator of (74) were replaced by sums

$$\sum[I_{\pi,d}]\sigma(pn\pi^+\pi^-)N(T_n)\Delta T_n, \quad (77)$$

with $\Delta T_n=0.2$ Bev. There are six terms in each sum, which correspond to $T_n=1.1$, 1.3, 1.5, 1.7, 1.9, and 2.1 Bev. At each energy $\sigma(pn\pi^+\pi^-)$ was evaluated by means of (73), (75), and (76). In order to obtain $I_{\pi,d}$ at these energies for the integral in the numerator, the curves of $I_{\pi,d}$ calculated for 1.0, 1.5, and 2.3 Bev were interpolated (see Fig. 4). We note that in Eq. (74), it is assumed that the values of $I_{\pi,d}$ at the different energies T_n have been normalized to the same area, i.e.,

$$\int_0^{\bar{T}_{\pi,m}} I_{\pi,d}d\bar{T}_\pi=\text{constant}. \quad (77a)$$

This is necessary, in order that the number of events at the different energies T_n will be proportional to $N(T_n)\sigma(pn\pi^+\pi^-)$.

The resulting pion momentum spectrum $\bar{v}_\pi\langle I_{\pi,d}\rangle$ is shown in Fig 17, together with the experimental results and the curve obtained from the statistical theory.[4] It may be noted that Fowler *et al.*[6] published two histograms for the energy distribution of the incident neutrons. Their spectrum A includes some ambiguous events, while spectrum B consists only of the selected events for which all momenta could be measured. The curve of $\bar{v}_\pi\langle I_{\pi,d}\rangle$ in Fig. 17 is based on spectrum B. However, it was found that if spectrum A is used instead, the resulting values of $\bar{v}_\pi\langle I_{\pi,d}\rangle$ are closely the same as those shown in Fig. 17 (the maximum difference is $\sim 3\%$), so that $\bar{v}_\pi\langle I_{\pi,d}\rangle$ is quite insensitive to the uncertainty in the incident neutron spectrum.

Figure 17 shows that the $\bar{v}_\pi\langle I_{\pi,d}\rangle$ curve from the isobar model gives a reasonable fit to the experimental pion spectrum, although it appears that the Fermi statistical theory gives slightly better agreement. We

[23] Chen, Leavitt, and Shapiro, Phys. Rev. **103**, 211 (1956).

believe that this is to a large extent fortuitous. Essentially the same comments apply as for the pion spectrum from single production at 0.8 Bev (Sec. V). The median incident neutron energy in the n-p experiment[6] is 1.7 Bev. The corresponding total energy $\bar{E}$ in the c.m.s. is 2.590 Bev. If $\bar{E}$ is equally divided between the two isobars, the maximum mass m_1 is 1.295 Bev, which is approximately equal to the cutoff $m_1=1.303$ Bev for single production at 0.8 Bev. In similarity to the single production results at 0.8 Bev, the maximum of the $d\sigma/d\bar{p}_\pi$ curve from the isobar model occurs at a momentum fairly close to the cutoff, since the effective maximum value of the isobar mass is not far above the resonance value (1.22 Bev). On the other hand, the spectrum given by the statistical theory will always have its maximum near the maximum momentum, by virtue of the $\bar{p}_\pi^2$ factor which is dominant, except near the upper end of the spectrum, where the decreasing momenta of the recoil nucleons begin to play a significant role. As is shown by Fig. 17, the maximum of the isobar curve occurs at $\bar{p}_\pi=220$ Mev/c, which is actually equal to the value of p_π^* of the pion in the rest system of an isobar of mass $m_1=1.22$ Bev, corresponding to the center of the resonance. Fortuitously the maximum of the Fermi curve agrees with this value. However, if the average incident neutron energy were increased, the maximum of the isobar model curve would not shift appreciably, whereas the maximum of the Fermi spectrum would be at a considerably higher momentum.

Fowler *et al.*[6] have obtained the following ratios for the number of $pn\pi^+\pi^-$, $pp\pi^0\pi^-$, and $pp\pi^-$ events:

$$(pn\pi^+\pi^-)/(pp\pi^0\pi^-)/(pp\pi^-) = (3.2\pm0.7)/(1\pm0.35)/(0.8\pm0.3).$$

In the present model, these ratios are given by $\langle\sigma(pn\pi^+\pi^-)\rangle/\langle\sigma(pp\pi^0\pi^-)\rangle/\langle\sigma(pp\pi^-)\rangle$ where

$$\langle\sigma(pn\pi^+\pi^-)\rangle=\tfrac{1}{2}[(41/45)\langle\sigma_{d,\,T=1}\rangle+(5/9)\langle\sigma_{d,\,T=0}\rangle], \quad (78)$$

$$\langle\sigma(pp\pi^0\pi^-)\rangle=\tfrac{1}{2}[(1/45)\langle\sigma_{d,\,T=1}\rangle+\tfrac{1}{9}\langle\sigma_{d,\,T=0}\rangle], \quad (79)$$

$$\langle\sigma(pp\pi^-)\rangle=\tfrac{1}{12}\langle\sigma_{s,\,T=1}\rangle, \quad (80)$$

and where the $\langle\ \rangle$ signs denote an average over the incident neutron energy distribution, e.g.:

$$\langle\sigma_{d,\,T=1}\rangle=\frac{\int_{1.0\text{ Bev}}^{2.2\text{ Bev}}\sigma_{d,\,T=1}N(T_n)dT_n}{\int_{1.0\text{ Bev}}^{2.2\text{ Bev}}N(T_n)dT_n}. \quad (81)$$

In Eq. (80), $\sigma_{s,\,T=1}$ is the cross section for single production in the $T=1$ state; $\sigma_{s,\,T=1}$ was obtained from [see Eq. (75)]:

$$\sigma_{s,\,T=1}=26[S/(D+S)]\text{ mb}. \quad (82)$$

With the choice of $k=0.6$ made above, and using Eq. (76) for $\sigma_{d,\,T=0}$, one obtains $\langle\sigma_{d,\,T=1}\rangle=9.4$ mb, $\langle\sigma_{d,\,T=0}\rangle=17.3$ mb, and $\langle\sigma_{s,\,T=1}\rangle=16.6$ mb. The calculated ratios as given by Eqs. (78)–(80) are

$$(pn\pi^+\pi^-)/(pp\pi^0\pi^-)/(pp\pi^-)=8.54/1/1.30.$$

These results were obtained by means of the neutron spectrum B. However, the ratios would be practically unchanged if we had used spectrum A. (One obtains 8.53/1/1.28.) The calculated ratio of 8.54/1.30=6.57 for $(pn\pi^+\pi^-)/(pp\pi^-)$ is somewhat larger than the observed value of 4.0 ± 1.7. However, we note that at the incident energies of this experiment (1.0–2.2 Bev), the ratio of double to single production rises very rapidly with the incident energy, so that the calculated result depends very sensitively on the value of k assumed for the $T=1$ pion production and on the behavior of $\sigma_{d,\,T=0}$. The assumption (76) about $\sigma_{d,\,T=0}$ is admittedly only a crude approximation. Thus it is quite possible that not all of the difference $\sigma_{T=0}-17$ mb represents double pion production. Indeed it seems reasonable that the cross section for elastic scattering $\sigma_{e,\,T=0}$ will increase concurrently with the double production between 1.0 and 1.6 Bev, as a result of the diffraction effect. (If the nucleon area effective for pion production were completely black, the increase of $\sigma_{e,\,T=0}$ would be equal to the increase of $\sigma_{d,\,T=0}$.) Furthermore, the value $k=0.8$ (instead of 0.6) would still be consistent with the data on the multiplicity, as can be seen from Fig. 9. With $k=0.8$ and assuming that only half the rise of $\sigma_{T=0}$ represents double production, i.e.,

$$\sigma_{d,\,T=0}=\tfrac{1}{2}(\sigma_{T=0}-17\text{ mb}), \quad (83)$$

one finds: $\langle\sigma_{d,\,T=1}\rangle=7.9$ mb, $\langle\sigma_{d,\,T=0}\rangle=8.6$ mb, $\langle\sigma_{s,\,T=1}\rangle=18.1$ mb, giving $\langle\sigma(pn\pi^+\pi^-)\rangle/\langle\sigma(pp\pi^-)\rangle=3.95$, in very good agreement with the experimental value of 4.0 ± 1.7.

As has been pointed out by Fowler *et al.*,[6] the prediction oft he Fermi statistical theory would be

$$(pn\pi^+\pi^-)/(pp\pi^0\pi^-)/(pp\pi^-)=3.3/1/20.5.$$

The ratio 3.3/20.5=0.161 for $(pn\pi^+\pi^-)/(pp\pi^-)$ is more than 20 times smaller than the experimental value, thus giving far too little double production. By contrast, the present theory based on the isobar model is able to give a good general agreement with the anomalously large ratio of double to single production observed in this experiment.

VII. ANGULAR CORRELATIONS BETWEEN PIONS AND NUCLEONS

The isobar model of pion production predicts a definite angular correlation between the pions produced and the recoil nucleons. The correlation effects are especially marked at relatively low bombarding energies ($T_p\lesssim1$ Bev) for which the excited nucleon N^* has a low velocity in the c.m.s. In the following, we will therefore restrict ourselves to the case of single N^*

production. We will consider first the correlation effects in p-p collisions.

In the extreme case, at threshold, where the final N and N^* are at rest in the c.m.s., one expects that the pion should be made at 180° with respect to the nucleon from the N^* decay and should not be correlated in direction with the unexcited nucleon. In the following, these two angular correlations will be represented by the functions C_1 and C_2, respectively.

C_1 gives the correlation between the decay products of the isobar. The expression for C_1 has been derived previously.[24] If C_1 denotes the number of events per unit solid angle, one finds

$$C_1=\frac{dn}{\sin\bar{\alpha}d\bar{\alpha}}=\frac{m_1}{2p_1p_\pi^*}\left|\sec\bar{\alpha}\Big/\left[\frac{\bar{E}_\pi\bar{E}_N-B}{\bar{E}_\pi\bar{E}_N-B}+\frac{\bar{E}_\pi}{\bar{E}_\pi^2-m_\pi^2}-\frac{\bar{E}_N}{\bar{E}_N^2-m_N^2}\right]\right|, \quad (84)$$

where $\bar{\alpha}$ is the c.m.s. angle between the pion and nucleon, p_π^* is the pion momentum in the rest system of m_1, $\bar{E}_\pi$ and $\bar{E}_N$ are the total c.m.s. energies of the pion and nucleon respectively, m_N=nucleon mass. B is defined as

$$B\equiv\tfrac{1}{2}(m_1^2-m_N^2-m_\pi^2). \quad (84a)$$

The angle $\bar{\alpha}$ is related to $\bar{E}_\pi$ and $\bar{E}_N$ by

$$\cos\bar{\alpha}=(\bar{E}_\pi\bar{E}_N-B)/[(\bar{E}_\pi^2-m_\pi^2)^{\frac{1}{2}}(\bar{E}_N^2-m_N^2)^{\frac{1}{2}}]. \quad (85)$$

Equation (84) pertains to a particular value of the isobar mass m_1, and must still be averaged over all possible values of m_1. This average is given by

$$\bar{C}_1(\bar{\alpha})=\frac{\int_{M_a}^{M_{1,s}}\sigma(m_1)FC_1(\bar{\alpha})dm_1}{\int_{M_a}^{M_{1,s}}\sigma(m_1)Fdm_1}, \quad (86)$$

where the notation is the same as in Eq. (9).

The function C_2 gives the correlation of the pion with the unexcited nucleon. Since the direction of this nucleon is opposite to the direction of the isobar N^*, C_2 is equal to the Jacobian for the two-body decay, as given by Eq. (29), in which $\theta_\pi=180°-\bar{\alpha}$, where $\bar{\alpha}$ is the angle between pion and nucleon in the c.m.s. C_2 must be averaged over m_1 in the same manner as C_1 [see Eq. (86)]. The resulting average will be called $\bar{C}_2$.

We will first consider the correlation between π^+-mesons and protons. The term $\frac{3}{4}\psi_{\frac{3}{2}}^2\eta_{-\frac{1}{2}}^2$ in the density [Eq. (44)] gives a fraction $\frac{3}{4}$ of (π^+,p) pairs arising from N^* decay. The term $\frac{1}{4}\psi_{\frac{1}{2}}^2\eta_{\frac{1}{2}}^2$ similarly yields a fraction $(\frac{1}{4})(\frac{1}{3})=\frac{1}{12}$ of (π^+,p) pairs in which the proton was not excited. Hence the complete correlation function, to be called $\bar{C}_{p-p}(\pi^+,p)$ is given by

$$\bar{C}_{p-p}(\pi^+,p)=\tfrac{3}{4}\bar{C}_1+\tfrac{1}{12}\bar{C}_2. \quad (87)$$

For the (π^+,n) correlation, the term $\frac{3}{4}\psi_{\frac{3}{2}}^2\eta_{-\frac{1}{2}}^2$ contributes $\frac{3}{4}\bar{C}_2$, and $\frac{1}{4}\psi_{\frac{1}{2}}^2\eta_{\frac{1}{2}}^2$ gives $\frac{1}{12}\bar{C}_1$, so that

$$\bar{C}_{p-p}(\pi^+,n)=\tfrac{1}{12}\bar{C}_1+\tfrac{3}{4}\bar{C}_2. \quad (88)$$

Similarly, one finds for (π^0,p)

$$\bar{C}_{p-p}(\pi^0,p)=\tfrac{1}{6}(\bar{C}_1+\bar{C}_2). \quad (89)$$

We note that for the (π^+,p) and (π^+,n) cases, the roles of $\bar{C}_1$ and $\bar{C}_2$ are interchanged. For $\bar{C}_{p-p}(\pi^+,p)$, the correlation is mostly of the type $\bar{C}_1$, partly because the $\psi_{\frac{3}{2}}^2$ density has a large coefficient $(\frac{3}{4})$, and also because the $\psi_{\frac{1}{2}}^2$ density gives only a fraction $\frac{1}{3}$ of π^+ (as compared to $\frac{2}{3}$ for π^0). It may be remarked that the angular correlation is, of course, completely determined by the ratio of the coefficients of $\bar{C}_1$ and $\bar{C}_2$. The values of the coefficients of Eqs. (87)–(89) correspond to the relative number of (π^+,p), (π^+,n) and (π^0,p) pairs expected from the present isobar model.

For single N^* production in n-p collisions, one finds from Eqs. (39), (40), and (59)

$$\bar{C}_{n-p}(\pi^+,n)=\bar{C}_{n-p}(\pi^-,p)=\tfrac{1}{6}(\bar{C}_1+\bar{C}_2), \quad (90)$$

$$\bar{C}_{n-p}(\pi^0,p)=\bar{C}_{n-p}(\pi^0,n)=\tfrac{1}{3}(\bar{C}_1+\bar{C}_2). \quad (91)$$

In this case the angular correlation is the same for all types of pion-nucleon pairs.

Figure 18 shows the partial correlation functions $C_1(\bar{\alpha})$ at T_p=0.8 Bev for m_1=1.10, 1.15, 1.20, 1.225, 1.25, and 1.275 Bev. It is seen that the general behavior of the curves of C_1 changes rapidly as m_1 is increased. For m_1=1.10 Bev, the distribution has its maximum at $\bar{\alpha}\cong45°$ and decreases rapidly for $\bar{\alpha}>70°$, as a result of the motion of the isobar, which tends to reduce the angle $\bar{\alpha}$ between pion and nucleon. As m_1 is increased, the velocity $\bar{v}_1$ of the isobar decreases, so that it is more likely that the pion and nucleon will be emitted at a large relative angle $\bar{\alpha}\gtrsim90°$. For $m_1\gtrsim1.24$ Bev, $\bar{v}_1$ is

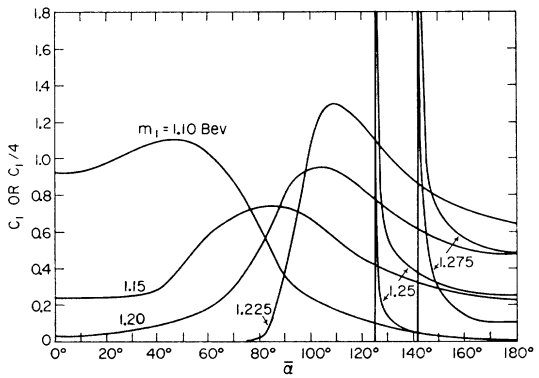

FIG. 18. Partial correlation functions C_1 for various values of m_1 for T_p=0.8 Bev. For $m_1\leqq1.225$ Bev, the curves give C_1 directly; for m_1=1.25 and 1.275 Bev, the values of $C_1/4$ have been plotted

[24] R. M. Sternheimer, Phys. Rev. **98**, 205 (1955). In Eqs. (8) and (9), $(E_1^2-m_1^2)^{\frac{1}{2}}$ and $(E_2^2-m_2^2)^{\frac{1}{2}}$ should be replaced by $E_1^2-m_1^2$ and $E_2^2-m_2^2$, respectively. For the results given in Fig. 1, the correct expression for $dn/d\theta$ was used.

less than the velocity v_N^* of the nucleon in the rest system of the isobar. As a result there is a minimum possible angle[24] $\bar{\alpha}_m$ which is larger than 90°, and the distribution $C_1(\bar{\alpha})$ has two branches between $\bar{\alpha}_m$ and 180°, as shown in Fig. 18 for $m_1=1.25$ and 1.275 Bev. The total $C_1(\bar{\alpha})$ is given by the sum of the terms due to the two branches. Of course, for the maximum possible m_1 (=1.30 Bev at $T_p=0.8$ Bev), $C_1(\bar{\alpha})$ is zero everywhere except at 180°, since the isobar is made at rest in the c.m.s. In the calculation of the weighted average $\bar{C}_1(\bar{\alpha})$, we used values of $C_1(\bar{\alpha})$ at intervals of 25 Mev from $m_1=1.10$ to $m_1=1.20$ Bev, and at intervals of 12.5 Mev between $m_1=1.20$ and 1.30 Bev.

The partial correlation functions $C_2(\bar{\alpha})$ for $T_p=0.8$ Bev are shown in Fig. 19. It is seen that the curves of $C_2(\bar{\alpha})$ have a pronounced backward maximum. This maximum is entirely due to the motion of the isobar, since for an isobar at rest, all decay angles would be equally probable, and C_2 would be constant (=0.5).

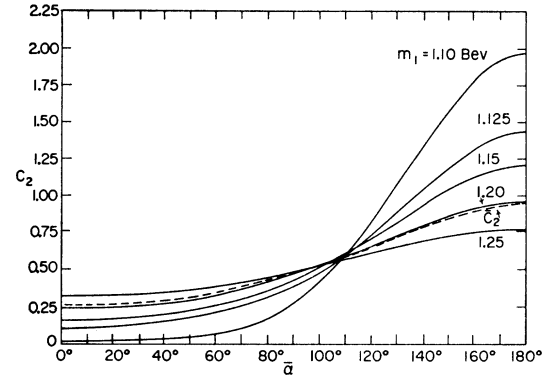

FIG. 19. Partial correlation functions C_2 for various values of m_1 for $T_p=0.8$ Bev. The dashed curve gives the average correlation function $\bar{C}_2$.

Figure 19 also shows that the weighted average $\bar{C}_2$ is very close to the function C_2 for $m_1=1.20$ Bev. This result was also verified for other values of the incident energy T_p, and arises from the fact that the weighting factor $\sigma(m_1)F$ has its maximum at ~1.20 Bev. Since the shape of the C_2 curves does not vary rapidly with m_1 in this region, the 1.20-Bev curve predominates and essentially determines the behavior of $\bar{C}_2$.

Calculations of $\bar{C}_1$ and $\bar{C}_2$ have been carried out at $T_p=0.8$ and 1.5 Bev for comparison with the Brookhaven cloud-chamber data[7] at these energies. The functions $\bar{C}(\pi^+,p)$ and $\bar{C}(\pi^+,n)$ in these comparisons were taken as normalized to unity. They are given by

$$\bar{C}(\pi^+,p)=0.9\bar{C}_1+0.1\bar{C}_2, \quad (92)$$

$$\bar{C}(\pi^+,n)=0.1\bar{C}_1+0.9\bar{C}_2, \quad (93)$$

so that $\int_0^\pi \bar{C}(\pi^+,N)\sin\bar{\alpha}d\bar{\alpha}=1$.

Figure 20 shows the curves of $\bar{C}(\pi^+,p)$ and $\bar{C}(\pi^+,n)$ for 0.8 Bev, together with the histogram of the distributions of (π^+,p) and (π^+,n) angles observed in the experiment

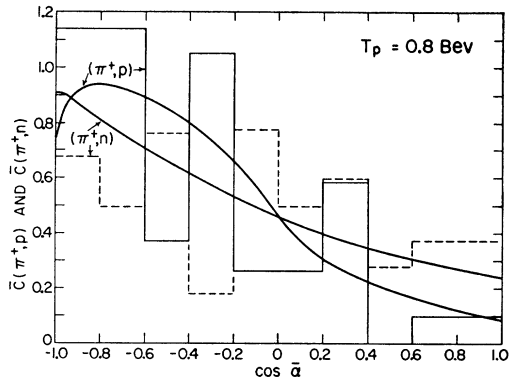

FIG. 20. Distributions $\bar{C}(\pi^+,p)$ and $\bar{C}(\pi^+,n)$ of the values of $\cos\bar{\alpha}$ for (π^+,p) and (π^+,n) pairs at $T_p=0.8$ Bev. The solid curves were obtained from the isobar model [Eqs. (92) and (93)]. The histograms represent the experimental data on $pn\pi^+$ events of Morris, Fowler, and Garrison [reference 7(I)] [solid lines: (π^+,p); dashed lines: (π^+,n)]. All of the curves and histograms are normalized to the same area.

of Morris, Fowler, and Garrison [reference 7(I)] at this energy. The (π^+,p) histogram is given by the full lines, while the (π^+,n) histogram is shown by the dashed lines; both have been normalized to the same area (=1) as the theoretical curves. The histograms of Fig. 20 pertain to the "selected" events of Morris *et al.* [reference 7(I)] (see Fig. 7 of their paper) for which particularly precise measurements could be made. It is seen that the theoretical curve of $\bar{C}(\pi^+,p)$ is in reasonable agreement with the experimental backward peak of the (π^+,p) distribution. The distribution of (π^+,n) angles also has a backward maximum, i.e., more cases with $\bar{\alpha}>90°$ than with $\bar{\alpha}<90°$ (the ratio of the number of these events is 58:42). However, the backward maximum is not as prounced as for (π^+,p). In agreement with this feature, the calculated (π^+,n) curve has less area in the backward hemisphere than that for (π^+,p).

Figure 20 shows that the maximum of $\bar{C}(\pi^+,p)$ is at ~145°, rather than at 180°, as would be expected for an isobar at rest in the c.m.s. This result is due to the behavior of C_1, as has been discussed above. Thus it is seen from Fig. 18 that the maxima of the curves of C_1 for $m_1=1.20$ and 1.225 Bev (~resonance energy) occur at 100°–110°. Similarly, the functions C_1 for $m_1=1.25$ and 1.275 Bev, for which the weighting factor $\sigma(m_1)F$ is also very large, have their maxima well below 180°. Thus $\bar{C}_1$, which is the weighted average of the C_1, has its maximum at ~145° and the location of this maximum essentially determines that of $\bar{C}(\pi^+,p)$.

Figure 21 shows the functions $\bar{C}(\pi^+,p)$ and $\bar{C}(\pi^+,n)$ for $T_p=1.5$ Bev, together with the histogram of the experimental distributions obtained by Fowler, Shutt, Thorndike, and Whittemore [reference 7(II)]. Because of the limited statistics, we have used all of the cases which have been interpreted by Fowler *et al.* [reference 7(II)] as $pn\pi^+$ events (see Fig. 5 of their paper). This group includes some ambiguous events, some of which may have been cases of double production. Fowler *et al.*

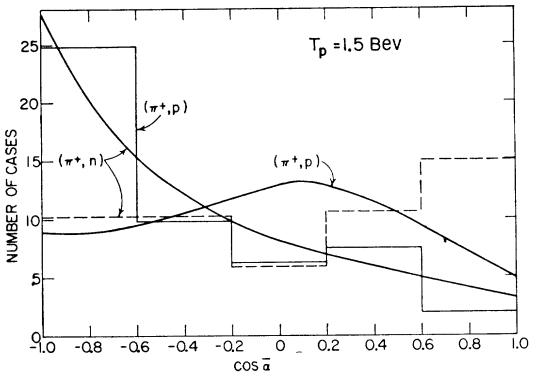

FIG. 21. Distributions $\bar{C}(\pi^+,p)$ and $\bar{C}(\pi^+,n)$ of the values of $\cos\bar{\alpha}$ for (π^+,p) and (π^+,n) pairs at $T_p=1.5$ Bev. The full curves were obtained from the isobar model [Eqs. (92) and (93)]. The histograms represent the experimental data on $pn\pi^+$ events of Fowler, Shutt, Thorndike, and Whittemore [reference 7(II)] [solid lines: (π^+,p); dashed lines: (π^+,n)]. The theoretical curves are normalized to the number of observed events.

[reference 7(II)] have plotted their histograms using intervals of 0.2 in $\cos\bar{\alpha}$. Some of their angular regions contain only 1 or 2 events. We have therefore combined their results for adjacent regions, and Fig. 21 shows the resulting histogram with intervals of 0.4 for $\cos\bar{\alpha}$. In each case, the theoretical curve of $\bar{C}(\pi^+,p)$ or $\bar{C}(\pi^+,n)$ has been normalized to the number of observed events. The calculation of $\bar{C}(\pi^+,N)$ proceeds in the same manner as for 0.8 Bev, except that at 1.5 Bev, all values of m_1 up to $M_b=1.58$ Bev are possible.

It is seen from Fig. 21 that the calculated curves for $\bar{C}(\pi^+,N)$ are in poor agreement with the experimental histograms. Thus for (π^+,p), the experimental distribution has a peak for $\bar{\alpha}$ near 180° ($-1<\cos\bar{\alpha}<-0.6$), consisting of 25 events, whereas the theoretical curve would give only 9 events, which is too low by ~3 standard deviations. On the other hand, for (π^+,n) in the same region of $\bar{\alpha}$, the calculated curve has an average value of 20, whereas only 10 events are observed. It should be noted that the angular correlation depends sensitively on the detailed assumptions of the present model. Thus it is assumed that the N^* decays as a free particle, independent of the unexcited nucleon N. However, if there is some interaction between the N^* and N, this would tend to distort the angular distributions of the pions given by the Jacobian for the free decay. In this connection, we note that all of the other predictions of the isobar model at 1.5 Bev are in reasonably good agreement with the experimental results of Fowler *et al.* [reference 7(II)] (pion and recoil nucleon momentum spectra, see Figs. 14 and 15; Q-value distribution, see Fig. 23, below). As was mentioned above, the experimental results may include some cases of double pion production, presumably $pn\pi^+\pi^0$ events. This may be responsible for the observed peak of the (π^+,p) distribution at $\bar{\alpha}\sim180°$. If two pions are produced, the available kinetic energy in the c.m.s. is decreased quite appreciably, from 500 to 360 Mev. For the $pn\pi^+\pi^0$ events, the velocity of each isobar N^* is therefore considerably smaller, on the average, than that of the single N^* produced in the $pn\pi^+$ cases. As a result, the proton and π^+ tend to come out more nearly at 180° with respect to each other. Thus it is possible that the peak of the observed (π^+,p) angular distribution at 180° may be due in part to the inclusion of some $pn\pi^+\pi^0$ events. It should also be noted that the statistical uncertainties may be responsible for at least part of the discrepancy.

VIII. EFFECTIVE Q VALUES FOR PION-NUCLEON PAIRS

In previous discussions of the experimental data on pion production at Cosmotron energies the concept of an effective Q value for pion-nucleon pairs has been extensively used. The Q value is defined as

$$Q\equiv\bar{E}_{\pi N}-(m_N+m_\pi), \tag{94}$$

where $\bar{E}_{\pi N}$ is the total energy of the pion and nucleon in the center-of-mass system of the two particles.

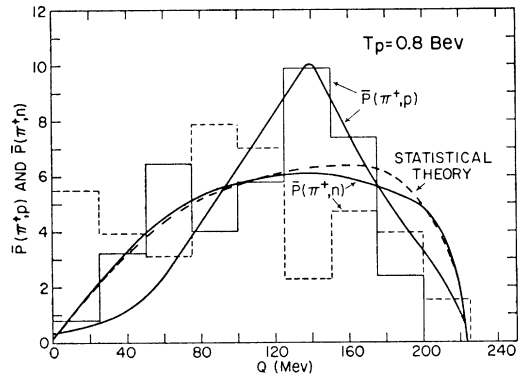

FIG. 22. Distributions $\bar{P}(\pi^+,p)$ and $\bar{P}(\pi^+,n)$ of Q values of (π^+,p) and (π^+,n) pairs at $T_p=0.8$ Bev. The solid curves were obtained from the isobar model [Eqs. (99) and (100)]. The histograms represent the experimental data on $pn\pi^+$ events of Morris, Fowler, and Garrison [reference 7(I)] [solid lines: (π^+,p); dashed lines: (π^+,n)]. The dashed curve gives the result of the Fermi statistical theory.[21] All of the curves and histograms are normalized to the same area.

From the point of view of the present model, there are two types of pion-nucleon pairs at the proton energies for which single N^* production predominates. Thus the nucleon may have originated from the isobar N^* which decays into the pion, or it may not have been excited in the collision. The probability distributions of the Q values for these two types of pairs will be denoted by $\bar{P}_1(Q)$ and $\bar{P}_2(Q)$, respectively.

In the present model, $\bar{P}_1(Q)$ is given by

$$\bar{P}_1(Q)=\sigma(m_1)F\Big/\int_{M_a}^{M_{1,s}}\sigma(m_1)Fdm_1, \tag{95}$$

where $m_1=m_N+m_\pi+Q$. Here F is the phase space factor and the denominator merely ensures that $\bar{P}_1(Q)$ is

normalized to 1, i.e., $\int_0^{Q_m}\bar{P}_1(Q)dQ=1$, where Q_m is the maximum possible Q for the energy T_p: $Q_m=M_{1,s}-(m_N+m_\pi)$.

In order to obtain the function $\bar{P}_2$ which pertains to the unexcited nucleon, we consider first an isobar with a definite mass m_1. The corresponding Q distribution which will be called P_2 was obtained as follows: For various angles of decay θ_π^* in the rest system of the isobar (at intervals of 22.5°), the energy and angle of the pion in the c.m.s. of the initial nucleons were calculated, and from these results the total energy $\bar{E}_{\pi N}$ in the center-of-mass system of the pion and the unexcited nucleon was obtained. The corresponding Q value is given by (94), and its relative probability is $\sin\theta_\pi^*$, since the solid angle available for a range $d\theta_\pi^*$ is $\sin\theta_\pi^* d\theta_\pi^*$. The values of θ_π^* considered in the calculation will be called $\theta_{\pi,i}^*$ ($\theta_{\pi,1}^*=0°$, $\theta_{\pi,2}^*=22.5°$, $\cdots$, $\theta_{\pi,9}^*=180°$). Let Q_i be the Q value pertaining to $\theta_{\pi,i}^*$. We define

$$Q_i^{(-)}\equiv\tfrac{1}{2}(Q_{i-1}+Q_i), \tag{96}$$

$$Q_i^{(+)}\equiv\tfrac{1}{2}(Q_i+Q_{i+1}). \tag{96a}$$

P_2 is given by

$$P_{2,i}=\frac{\sin\theta_{\pi,i}^*}{Q_i^{(+)}-Q_i^{(-)}}\left[1\Big/\sum_{i=1}^{9}\sin\theta_{\pi,i}^*\right], \tag{97}$$

for $Q_i^{(-)}<Q<Q_i^{(+)}$. The factor in the square bracket serves merely to normalize the distribution. $P_{2,i}$ as defined by (97) gives a series of step functions. A smooth curve is drawn through these step functions in obtaining the final function $P_2(Q)$, which, of course, still depends on m_1.

Contrary to $\bar{P}_1$ [Eq. (95)] which has a pronounced peak at $Q\approx145$ Mev ($m_1\approx1.22$ Bev), the functions $P_2(Q)$ for the various m_1 are almost constant over the range Q, except near $Q=0$ and the maximum Q. The average $\bar{P}_2$ over the values of m_1 is given by

$$\bar{P}_2(Q)=\frac{\int_{M_a}^{M_{1,s}}P_2(Q)\sigma(m_1)F dm_1}{\int_{M_a}^{M_{1,s}}\sigma(m_1)F dm_1}. \tag{98}$$

The distribution $\bar{P}$ for (π^+,p) and (π^+,n) pairs from p-p collisions is given by the following expressions similar to (92) and (93):

$$\bar{P}(\pi^+,p)=0.9\bar{P}_1+0.1\bar{P}_2, \tag{99}$$

$$\bar{P}(\pi^+,n)=0.1\bar{P}_1+0.9\bar{P}_2. \tag{100}$$

With this definition, the functions $\bar{P}(\pi^+,N)$ are normalized to unity:

$$\int_0^{Q_m}\bar{P}(\pi^+,N)dQ=1, \tag{100a}$$

where Q is in Bev.

Figure 22 shows $\bar{P}(\pi^+,p)$ and $\bar{P}(\pi^+,n)$ for $T_p=0.8$ Bev, together with the histograms of the experimental Q value distributions obtained by Morris, Fowler, and Garrison [reference 7(I)]. The full lines represent the (π^+,p) values, while the broken lines give the (π^+,n) histogram. Similarly to the distribution of $\bar{\alpha}$ values at 0.8 Bev, we have used only the "selected" events in the experimental histograms, which are normalized to the same area as the theoretical curves. It is seen that the calculated curve for $\bar{P}(\pi^+,p)$ is in good agreement with the peak of the experimental histogram at 140 Mev. The narrow maximum of $\bar{P}(\pi^+,p)$ reflects, of course, the behavior of $\bar{P}_1$, which reproduces essentially the scattering cross section $\sigma(m_1)$. By contrast, the function $\bar{P}(\pi^+,n)$ is relatively flat except near the ends of the distribution, as was expected from the behavior of P_2. This result is in agreement with the experimental histogram which does not exhibit any well-defined maximum. For comparison, we have also shown in Fig. 22 the normalized curve of $\bar{P}(\pi^+,N)$ expected from the statistical theory, as obtained by Block.[21] The statistical distribution [which is the same for (π^+,p) as for (π^+,n)] is in definite disagreement with the (π^+,p) histogram. Since, on the other hand, the isobar model gives good agreement with the observed peak, this result can be regarded as giving strong support for the isobar model at 0.8 Bev, and as evidence against the statistical theory.

Calculations of $\bar{P}(\pi^+,p)$ and $\bar{P}(\pi^+,n)$ have also been carried out for $T_p=1.5$ Bev. Figure 23 shows the comparison with the experimental histograms of the $pn\pi^+$ events obtained by Fowler, Shutt, Thorndike, and Whittemore [reference 7(II)]. Similarly to the distribution of angles $\bar{\alpha}$ at 1.5 Bev, we have used all of the $pn\pi^+$ events at this energy. The histograms may thus include a few cases of double production, as was pointed out by Fowler *et al.* [reference 7(II)]. It is

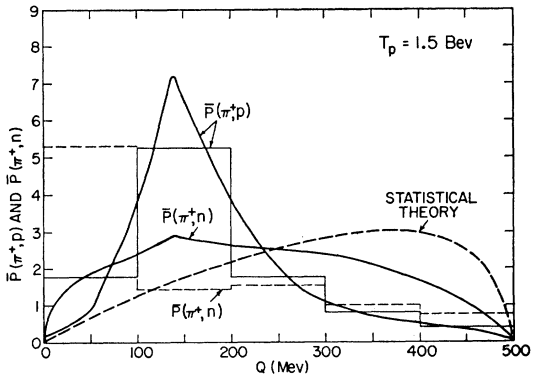

FIG. 23. Distributions $\bar{P}(\pi^+,p)$ and $\bar{P}(\pi^+,n)$ of Q values of (π^+,p) and (π^+,n) pairs at $T_p=1.5$ Bev. The solid curves were obtained from the isobar model [Eqs. (99) and (100)]. The histograms represent the experimental data on $pn\pi^+$ events of Fowler, Shutt, Thorndike, and Whittemore [reference 7(II)] [solid lines: (π^+,p); dashed lines: (π^+,n)]. The dashed curve gives the result of the Fermi statistical theory.[21] All of the curves and histograms are normalized to the same area.

seen that the calculated curve of $\bar{P}(\pi^+,p)$ is in very good agreement with the maximum of the experimental distribution between 100 and 200 Mev, thus giving strong support to the present isobar model. The curve of $\bar{P}(\pi^+,n)$ is quite flat throughout the region of Q which corresponds to the resonance, in agreement with the experimental distribution. However, the (π^+,n) histogram has a maximum for low Q values (between 0 and 100 Mev) which is not reproduced by the calculations. This maximum may be due in part to the inclusion of some double-pion events. It should also be noted that the statistics of the experiment were quite limited, so that not too much significance can be attached to this discrepancy. Thus of the 50 events which were used by Fowler *et al.* [reference 7(II)] in the histograms, only 19 were classified with certainty as being $pn\pi^+$ events. In Fig. 23, the prediction of the statistical theory[21] is shown for comparison. It is seen that this curve is in definite disagreement both with the (π^+,p) and (π^+,n) Q value distributions, since the maximum of the curve occurs at much too large Q values ($\sim$380 Mev) to give a fit to either the (π^+,p) or (π^+,n) data.

IX. ANGULAR DISTRIBUTION OF THE ISOBAR

It is of interest to observe that the angular dependence of the cross section for producing the isobar N^* can be inferred from the angular distribution of the pions, particularly in the case of single production where only one isobar is made. We shall write

$$a(\bar{\theta}_{N^*})=\sum_l a_l P_l(\cos\bar{\theta}_{N^*}) \tag{101}$$

for the angular distribution of N^*; $\bar{\theta}_{N^*}$ is the c.m.s. angle between the direction of N^* and that of the incident nucleon; the a_l are coefficients and P_l is the Legendre polynomial. For p-p collisions, where the initial system is symmetric with respect to 90° in the c.m.s., the distribution $a(\bar{\theta}_{N^*})$ must also be symmetric with respect to 90°, so that $a_l=0$ for odd l. For n-p collisions, the same property is expected to hold, provided that the strong interaction responsible for producing the isobar is not influenced by the respective initial charge states of the two nucleons, but is determined solely by the total isotopic spin T. The angular distribution of the pions will be denoted by $b(\bar{\beta}_\pi)$. We have

$$b(\bar{\beta}_\pi)=\sum_l b_l P_l(\cos\bar{\beta}_\pi), \tag{102}$$

where the b_l are coefficients; $\bar{\beta}_\pi$ is the c.m.s. angle of the pion with respect to the incident nucleon. We will consider first an isobar of a given mass m_1. The distribution $b(\bar{\beta}_\pi)$ is given by

$$b(\bar{\beta}_\pi)=\int_0^\pi\int_0^{2\pi}[\textstyle\sum_l a_l P_l(\cos\bar{\theta}_{N^*})]J \times\sin\bar{\theta}_{N^*}d\bar{\theta}_{N^*}d\bar{\varphi}_{N^*}, \tag{103}$$

where $\bar{\varphi}_{N^*}$ is the azimuthal angle of the isobar; J is the Jacobian for the decay of the isobar, as given by Eq. (29). It is assumed here that the isobar decays isotropically in its rest system.[19] J is a function of the angle $\bar{\theta}_\pi$ between the N^* and the emitted pion. In fact, $J(\bar{\theta}_\pi)=C_2(180°-\bar{\theta}_\pi)$, where C_2 is the correlation function introduced in Sec. VII. Upon expanding J in terms of Legendre polynomials, we obtain

$$J(\bar{\theta}_\pi)=\textstyle\sum_\lambda c_\lambda P_\lambda(\cos\bar{\theta}_\pi), \tag{104}$$

where the c_λ are coefficients. In order to carry out the integration of (103), we note that $\cos\bar{\theta}_\pi$ is given by Eq. (11). From the addition theorem for P_λ, we have

$$P_\lambda(\cos\bar{\theta}_\pi)=P_\lambda(\cos\bar{\beta}_\pi)P_\lambda(\cos\bar{\theta}_{N^*}) +2\sum_{m=1}^{\lambda}\frac{(\lambda-m)!}{(\lambda+m)!}P_\lambda^m(\cos\bar{\beta}_\pi) \times P_\lambda^m(\cos\bar{\theta}_{N^*})\cos[m(\bar{\varphi}_{N^*}-\bar{\varphi}_\pi)]. \tag{105}$$

In the integral of Eq. (103), the sum over m of (105) makes no contribution. Furthermore from the orthogonality and normalization of the P_l one finds

$$b(\bar{\beta}_\pi)=4\pi\textstyle\sum_l a_l c_l P_l(\cos\bar{\beta}_\pi)/(2l+1). \tag{106}$$

Upon equating (102) and (106), one obtains

$$a_l=(2l+1)b_l/4\pi c_l, \tag{107}$$

which gives the coefficients of the angular distribution of N^* in terms of the angular distribution of the emitted pions.

The preceding discussion has been restricted to isobars of a given fixed mass m_1. However, in the present model, the N^* can have a range of different masses m_1 with relative probability $\sigma(m_1)F$, where F is the phase space factor. We will assume for simplicity that the isobars of different mass are all made with the same angular distribution. In this case, Eq. (103) still holds for the complete range of masses, provided that J is replaced by the weighted average $\bar{J}$ over the mass values m_1:

$$\bar{J}=\int_{M_a}^{M_{1,s}}J\sigma(m_1)Fdm_1\Big/\int_{M_a}^{M_{1,s}}\sigma(m_1)Fdm_1. \tag{108}$$

As pointed out above, $J(\bar{\theta}_\pi)$ is given by the partial correlation function C_2 evaluated for $\bar{\alpha}=180°-\bar{\theta}_\pi$. Comparison of (108) with Eq. (86) shows that $\bar{J}$ is related in the same manner to the average correlation function $\bar{C}_2$. Thus $\bar{J}(\bar{\theta}_\pi)=\bar{C}_2(180°-\bar{\theta}_\pi)$. It can be concluded that Eq. (107) holds for the complete m_1 distribution (for single N^* production) provided that c_l is taken as the coefficient in the expansion of the average correlation function $\bar{C}_2$.

The preceding considerations have been applied to the data obtained for 0.8-Bev protons by Morris, Fowler, and Garrison [reference 7(I)]. Making use of the symmetry about $\bar{\beta}_\pi=90°$, Morris *et al.* [reference 7(I)] have folded their pion distributions about 90°

[see Fig. 4 of reference 7(I)]. The coefficients b_l of the expansion of $b(\bar{\beta}_\pi)$ are obtained from the expression

$$b_l=\tfrac{1}{2}(2l+1)\int_0^{\pi/2} b(\bar{\beta}_\pi)P_l(\cos\bar{\beta}_\pi)\sin\bar{\beta}_\pi d\bar{\beta}_\pi, \quad (109)$$

by integrating over the experimental histogram $b(\bar{\beta}_\pi)$. One thus obtains $b_0=1$, $b_2=0.915$, $b_4=-0.678$, so that

$$b(\bar{\beta}_\pi)\cong P_0+0.915P_2-0.678P_4. \quad (110)$$

It is doubtful whether the term in P_4 has much significance, in view of the uncertainties due to the limited statistics. Moreover, the first two terms of (110) give by themselves a reasonable fit to the experimental histogram. We will therefore disregard the P_4 term in the following discussion.

The average Jacobian $\bar{J}(\bar{\theta}_\pi)$ is given by $\bar{C}_2(180°-\bar{\theta}_\pi)$, where $\bar{C}_2$ is the function shown in Fig. 19. By integrating over $\bar{C}_2$ in a manner similar to Eq. (109), one finds $c_0=0.5$, $c_1=0.318$, $c_2=0.0929$, $c_3=0.0215$, so that

$$\bar{J}\cong 0.5P_0+0.318P_1+0.0929P_2+0.0215P_3. \quad (111)$$

This expression approximates $\bar{J}$ to within $\sim 1\%$. From (107), we now obtain $a_0=0.159$ and $a_2=3.92$, which gives

$$a(\bar{\theta}_{N^*})=0.159+3.92P_2=5.88\cos^2\bar{\theta}_{N^*}-1.80. \quad (112)$$

This result indicates that the distribution of N^* has a large $\cos^2\bar{\theta}_{N^*}$ component at 0.8 Bev. Equation (112) is, of course, not correct near 90°, where the expression becomes negative. This is due to the fact that the coefficient a_2 of the P_2 term is very large, and $P_2(90°)=-0.5$. As shown by (107), a_2 is proportional to b_2/c_2. The coefficient c_2 in the expansion of $\bar{J}$ is quite small (0.0929), so that any appreciable P_2 term in the experimental pion angular distribution will necessarily lead to a large value of a_2. The value $b_2=0.915$ obtained from the histogram [Eq. (110)] may be in excess of the actual value, because of statistical uncertainties. It should also be pointed out that the present treatment is based on the assumption that the isobar N^* decays as a free particle. It is possible that if the interaction of the N^* with the unexcited nucleon were taken into account, one would obtain a larger value of c_2 for the angular distribution from the decay, thus giving a smaller coefficient a_2. In any case, it can probably be concluded that the distribution of N^* has a pronounced forward-backward peak at 0.8 Bev. If the distribution is actually mainly proportional to $\cos^2\bar{\theta}_{N^*}$, this would imply that the N^* is produced in a p state. We note that the interpretation of the pion energy spectra of Lindenbaum and Yuan[3] in terms of the isobar model also gives an indication that the angular distribution of the isobar has a forward-backward maximum at 1.0 Bev, as was discussed in Sec. V.

X. SUMMARY AND CONCLUSIONS

An isobaric nucleon model for pion production in nucleon-nucleon collisions in the 0.8- to 3.0-Bev incident energy range has been presented. In this picture one or both of the incident colliding nucleons is considered excited to one of a series of possible isobaric levels. The $T'=J=\frac{3}{2}$ level previously observed in the $\pi-p$ scattering is assumed to be predominantly responsible for meson production in the energy range here considered, and is the only state introduced in the present treatment.

The isobar is considered to separate from the recoil nucleon or other isobar involved in the collision before decay and hence the decay of the isobar is treated independently of possible interactions between its decay products and the other particles in the collision. Several arguments involving estimated lifetime and other considerations have been previously made (see Sec. II) and tend to justify this assumption. However it is obvious that agreement or lack of agreement with experiment is the real test of the usefulness of the model.

The total isotopic spin and its z component are considered conserved throughout the process. In addition to isotopic spin the isobar is further characterized by the total energy of its decay products in its rest system or equivalently a mass in its rest system denoted by m_1. The relative probability for isobar formation in the range dm_1 was phenomenologically related to the π^++p interaction cross section. The probability for single isobar formation was taken proportional to $F\sigma(m_1)dm_1$, where F is the two body phase space factor for the final N^*+N state and $\sigma(m_1)$ is the appropriate π^+-p total interaction cross section. For double production (N^*+N^*), the probability was taken proportional to $F\sigma(m_1)\sigma(m_2)dm_1dm_2$.

Most of the calculations were performed for p-p interactions since most of the available data concerns this interaction. Furthermore in the p-p case only the isotopic spin=1 state is involved and the inelastic cross section for this state is known as a function of energy from 0.5 to 3.0 Bev. In the n-p case the $T=0$ inelastic cross section also enters. The total $T=0$ cross section is known; however, the separation of elastic from inelastic is uncertain.

The ratio of double to single plus double meson production in p-p collisions as a function of energy has been related to one dimensionless parameter k, which when fitted to experiment at one energy predicts a behavior of this ratio consistent with the experimental data available.

The angular distribution of the isobars in the c.m.s. was considered for the two cases of (1) an isotropic distribution and (2) forward and backward only. Mixtures of (1) and (2) can obviously be used to represent various degrees of forward and backward peaking. A more detailed angular distribution fit was

made to the available data for 0.8-Bev p-p interactions. The angular distribution of the decay products of the isobar in its own rest system was assumed isotropic. The angular distribution of the isobars has no effect on pion and nucleon energy or momentum spectra obtained by adding together all particles produced irrespective of angle. The cloud chamber data of reference 7 was of this form. However, in the case of observations of spectra at particular angles such as in the counter experiments of reference 3 the spectra at different angles are a function of this angular distribution.

All the experimental data on pion and nucleon spectra are in reasonable agreement with the model predictions. The observed angular distribution of the pions in the cloud chamber data implies some forward and backward peaking in the isobar angular distribution at 0.8 Bev. The counter experiments of reference 3 which corresponds to large angle (60°–90°) observations in the c.m.s. at 1.0 and 2.3 Bev are also consistent with some forward and backward peaking of the isobars at 1.0 Bev. However, the isotropic distribution seems to be a better approximation at 2.3 Bev.

The Fermi statistical theory predictions have been compared to the experimental data in this and also previous publications, and in general, do not agree. There is an apparent general agreement for the pion and nucleon energy and momentum spectra of the Fermi statistical theory, the present isobar model and the experimental data at 0.8 Bev.

However, at 1.0, 1.5, and 2.3 Bev the Fermi theory predictions do not agree with the experiments or the isobar model. This is true even if one arbitrarily mixes the predicted spectra for the Fermi theory single and double production, each of which is independent of the interaction volume, in a ratio determined by the experimental observations.

One should also recall at this point that the predicted branching ratios for the single and double production in the Fermi statistical theory depend on the interaction volume. For a volume equal to the Compton wavelength of the pion the double production estimate is much smaller than the observed value. Furthermore, the larger volume required to enhance double production corresponds to an inelastic cross-section estimate much more than double that observed.

The apparent agreement of the pion spectrum in the Fermi theory at 0.8 Bev with the isobar model predictions can be understood since there is not enough available energy to form the isobar beyond its peak energy. Hence one has a sharply rising probability of pion emission with increasing momentum much like the phase space factor in the Fermi theory. The nucleon spectra also agree coincidentally with the isobar model predictions.

At higher incident energies the effect of the sharp decrease of the resonance cross section above the peak in the isobar model enhances lower momentum pions at the expense of higher momentum pions, and also leads to enhanced double production when two isobars near the peak energy can be produced. Furthermore, the kinematics of the isobars are such that the average nucleon momenta at 1.5 Bev are higher than the Fermi theory predictions. This effect is also observed experimentally.

The apparent Q value between pions and nucleons has been calculated with the isobar model and compared to experimentally observed values and the Fermi statistical theory prediction. As in the case of the pion and nucleon momentum spectra, there is an apparent agreement in all three cases at 0.8 Bev. However, at 1.5 Bev the isobar model and the experiments generally agree but the Fermi theory disagrees because of too many high-energy cases.

The angular correlations for both pion and proton and pion and neutron pairs, have been calculated for 0.8 and 1.5 Bev.

They have been compared to the experimental data at 0.8 and 1.5 Bev, and are in general agreement with the observations at 0.8 Bev but do not agree at 1.5 Bev. In the latter case very poor statistics and the uncertainty of experimental errors do not make it possible to conclude whether a real disagreement exists.

The production of mesons in n-p collisions of average energy 1.7 Bev is described in reference 6. The observed result of much greater double production relative to single than in the case of p-p collisions has also been explained by the isobar model, since n-p contains a $T=0$ state in addition to the $T=1$ state of which p-p is exclusively composed. The inelastic cross section in the $T=0$ state must in the isobar model be composed only of double production, since it is impossible to combine one $T'=\frac{3}{2}$ isobar (for single production) with a $T'=\frac{1}{2}$ recoil nucleon to obtain a $T=0$ state. However, two $T'=\frac{3}{2}$ isobar states (for double production) can be combined to form a $T=0$ state.

An estimate of the $T=0$ inelastic cross section from the known total cross section gives the anomalously large amount of double production required to explain the observed greater abundance of this process in n-p collisions as compared to p-p collisions.

From the basic single and double pion production spectra, and various recoil nucleon spectra, one can by interpolating and compounding with the weighted coefficients given in the text obtain predictions for almost any pion production process in the 0.8- to 3.0-Bev range.

It is of interest to compare the present isobar model with the Kovacs[9] approach of modifying the Fermi statistical theory to include enhancement of various final states by the pion-nucleon interaction. Obviously there will be a certain general similarity of the two models due to the fact that the pion-nucleon interaction will tend to make the relative energy of pion and nucleon follow the scattering interaction as a function of energy, and this in turn will tend to simulate the isobar assumed in our model. However, there are several

marked differences involved, some of which are basic, and some of which were introduced by Kovacs in order to make the calculations possible.

Kovacs' phase space factors correspond to the multibody collections of two nucleons and one pion for single production and two nucleons and two pions for double production. Hence single production involves a three-body phase space and double production involves a four-body phase space. This approach is consistent with his picture of the process whereby in the first stage the various particles are created in a thermodynamic equilibrium with very strong mutual interactions which lead to effectively constant matrix elements for all states in this first stage of the process. Then he argues that the relatively longer range π-nucleon interaction results in a scattering of the outgoing pions by the nucleons and this interaction enhances those final states for which the scattering interaction is large.

In the isobar model all final states involve two bodies, either one nucleon and one isobar, or two isobars, for single or double pion production respectively.

Hence two-body phase space factors are used in all cases. Furthermore the resonance interaction is built into the moving isobars which can be quite energetic.

In Kovacs' case the nucleons are treated as S waves and nonrelativistically, and the pions are treated as P waves in the c.m.s.

This approach was applied mainly to predicting the behavior of the multiplicity and the ratios of various charge states as a function of energy in the 1.0- to 3.0-Bev range for p-p and n-p collisions. These results were in general agreement with experiment. However, except for one isolated case without experimental comparison, no calculations were performed for pion momentum spectra. No results for nucleon momentum spectra, Q values and angular correlations between pion-nucleon pairs were reported. Furthermore, it seems unlikely that this approximate treatment could properly treat the complicated dynamics involved in the case of fast moving nucleons at the higher energies, for which mesons emitted with a relative momentum corresponding to the resonant energy region tend to be enhanced. A more realistic treatment of these effects by the Kovacs model appears to be rather difficult.

The general quantitative agreement of the isobar model predictions and the considerable body of experimental data already available for the nucleon-nucleon production of pions in the 1.0- to 3.0-Bev range is most encouraging.

It seems clear that the major features of these interactions are well represented by this model. However the crudeness and lack of completeness of many of the experiments make it impossible at present to determine whether this model can also predict the finer details of these interactions.

An extensive investigation by counter techniques of pion production in p-p and n-p collisions at Cosmotron energies is now in progress[25] and should in the near future yield detailed results with which a more critical comparison can be made.

As previously mentioned the isobar model might well be applied to even higher energy pion production. In this case other isobars than the $T'=J=\frac{3}{2}$ state would most likely have to be included. Since the characteristics of such other isobars are not known and very little data on these higher energy interactions is available, it is not very fruitful to pursue this matter further at this time.

One other application of the isobar model would be in pion-nucleon collisions leading to pion production. This subject will be considered in a later publication.

ACKNOWLEDGMENTS

The authors are indebted to Dr. R. Serber for several helpful discussions and comments on this work.

We also wish to thank Dr. R. P. Shutt and his co-workers for giving us their experimental data prior to publication, and also for several valuable discussions.

[25] S. J. Lindenbaum and L. C. L. Yuan (private communication).